

Alma Mater Studiorum – Università di Bologna

DOTTORATO DI RICERCA IN
Biologia e Fisiologia Cellulare

Ciclo XXIV

Settore Concorsuale di afferenza: 05/E1

Settore Scientifico disciplinare: BIO10

Respiratory complex I dysfunction in tumorigenesis

Presentata da: Mariantonietta Capristo

Coordinatore Dottorato

Prof.ssa Michela Rugolo

Relatore

Prof.ssa Michela Rugolo

Correlatore

Dott.ssa Anna Maria Porcelli

Esame finale anno 2012

Summary

Abstract	3
Introduction	5
Mitochondria.....	6
The mitochondria ultrastructure.....	7
Mitochondrion matrix activity: β -oxidation and tricarboxylic acid cycle.....	9
The mitochondrial membrane oxidative phosphorylation.....	13
Mitochondrial DNA.....	16
Mitochondrial diseases.....	20
Mitochondrial metabolic dysfunction and cancer.....	23
Nuclear genes involved in mitochondrial defects in cancer.....	23
Mitochondrial genes involved in defective OXPHOS in cancer.....	26
Complex I: structure, assembly and function.....	31
Aims	38
Materials and methods	41
Results	48
Allotopic MTND1 expression strategy.....	49
Allotopic ND1 expression restores the energetic efficiency in cells bearing m.3571insC <i>ND1</i> mutation.....	50
ND1 allotopic expression rescues tumorigenic potential of OS-93 cell line.....	53
Complex I recovery by ND1 allotopic expression hampers oncocytic transformation.....	54
HIF1 α -stabilization is involved in increased tumor growth.....	56

Biochemical effect of ND1 allotopic expression is also preserved in <i>ex vivo</i> cell lines.....	57
Conclusion	61
References	67
Acknowledgements	89

Abstract

Diseases due to mutations in mitochondrial DNA probably represent the most common form of metabolic disorders, including cancer, as highlighted in the last years. Approximately 300 mtDNA alterations have been identified as the genetic cause of mitochondrial diseases and one-third of these alterations are located in the coding genes for OXPHOS proteins. Despite progress in identification of their molecular mechanisms, little has been done with regard to the therapy. Recently, a particular gene therapy approach, namely allotopic expression, has been proposed and optimized, although the results obtained are rather controversial. In fact, this approach consists in synthesis of a wild-type version of mutated OXPHOS protein in the cytosolic compartment and in its import into mitochondria, but the available evidence is based only on the partial phenotype rescue and not on the demonstration of effective incorporation of the functional protein into respiratory complexes. In the present study, we took advantage of a previously analyzed cell model bearing the m.3571insC mutation in *MTND1* gene for the ND1 subunit of respiratory chain complex I. This frame-shift mutation induces in fact translation of a truncated ND1 protein then degraded, causing complex I disassembly, and for this reason not in competition with that allotopically expressed. We show here that allotopic ND1 protein is correctly imported into mitochondria and incorporated in complex I, promoting its proper assembly and rescue of its function. This result allowed us to further confirm what we have previously demonstrated about the role of complex I in tumorigenesis process. Injection of the allotopic clone in nude mice showed indeed that the rescue of complex I assembly and function increases tumor growth, inducing stabilization of HIF1 α , the master regulator of tumoral progression, and consequently its downstream gene expression activation.

Introduction

MITOCHONDRIA

Mitochondria are eukaryotic subcellular organelles which play a crucial role in the energetic balance of the cell, since oxidative phosphorylation takes place in these compartments. This implies that mitochondria have a critical position between energy uptake (food uptake and metabolism) and energy production, and as a consequence, they are involved in many other cellular processes, like thermogenesis, apoptosis, oxygen reactive species production and calcium homeostasis.

Mitochondria show a complex double-membrane organization, where the outer membrane (OM) bounds the organelle, whereas the inner membrane (IM) separates the matrix space from the intermembrane space. The IM is organized in distinct structures, the peripheral inner membrane and the *cristae*, defined by several lines of evidence as the active site of oxidative phosphorylation (Perotti et al., 1983; D'Herde et al., 2001; Vogel et al., 2006), separated from peripheral inner membrane by narrow tubular structure called *cristae junctions* (Perkins et al., 2001; Frey et al., 2000).

In the cytosol, mitochondria form a highly dynamic reticulum, whose morphology depends on the cell types and context, and is due to the constant fusion/fission of both OM and IM (Chen et al., 2004, 2005; Liu et al., 2009). The ultrastructure and reticulum organization are determined by mitochondria-shaping proteins that regulate the equilibrium between fusion and fission process (Chen H et al., 2003).

A peculiar feature of mitochondria is the presence within the matrix of multiple copies of its own DNA, which encodes a small number of proteins that, with together those nucleus-coded ones, are essential for the energetic function (Anderson et al. 1981). In fact, mitochondrial function relies on the coordinate expression of two different genetic systems, the mitochondrial and the nuclear genome; however, it's the latter to encode the majority of proteins necessary to the organelle physiology, including those fundamental to expression and maintenance of the mitochondrial DNA (mtDNA).

A growing interest in mitochondria has been shown in recent years, due to implication of the mitochondrial dysfunction implication in human disorders. Many rare genetic pathologies are indeed caused by mutations in either mitochondrial DNA and nuclear genes that encode for mitochondrial proteins. Mitochondrial dysfunctions have been implicated also in more common human diseases, like neurodegenerative diseases,

cancers, diabetes and the natural process of ageing (Zeviani et al., 1997; Wallace 2005; Mao and Holt, 2009; Trifunovic, 2006).

The mitochondria ultrastructure

Mitochondria are double-membrane organelles; the OM is highly permeable because it contains many pores for small molecules, whereas the IM is impermeable to most small molecules and ions. This property is required to maintain an electrochemical gradient between the matrix and the intermembrane space (Nicholls et al., 2002). The IM folds into membrane inter-digitations, called *cristae* (Frey and Mannella, 2000), which increase their surface area and mass (Fig.1) and which represent a distinct element/compartiment extending into the mitochondrial interior like tubules or lamellae, and not as an unfolded membrane of the IM, as initially believed. The inner boundary membranes and the cristae are joined by a limited number of discrete sites called cristae junctions, which typically have a consistent diameter of 15-20 nm, but may be altered by matrix volume and respiratory activity (Frey et al., 2002; Frey and Mannella, 2000; Mannella et al., 1994; Mannella et al., 1997). It has been estimated that three quarters of the IM mass are proteins, and many of these are proteins of the oxidative phosphorylation (OXPHOS) system.

The matrix, interior of IM, is composed of a gel-like substance, which contains enzymes of the tricarboxylic acid (TCA) cycle or the Krebs cycle (Krebs and Johnson, 1937) and β -oxidation. These oxidation-reduction reactions and energy transfer processes make mitochondria the powerhouses of eukaryotic cells (Mao and Holt, 2009).

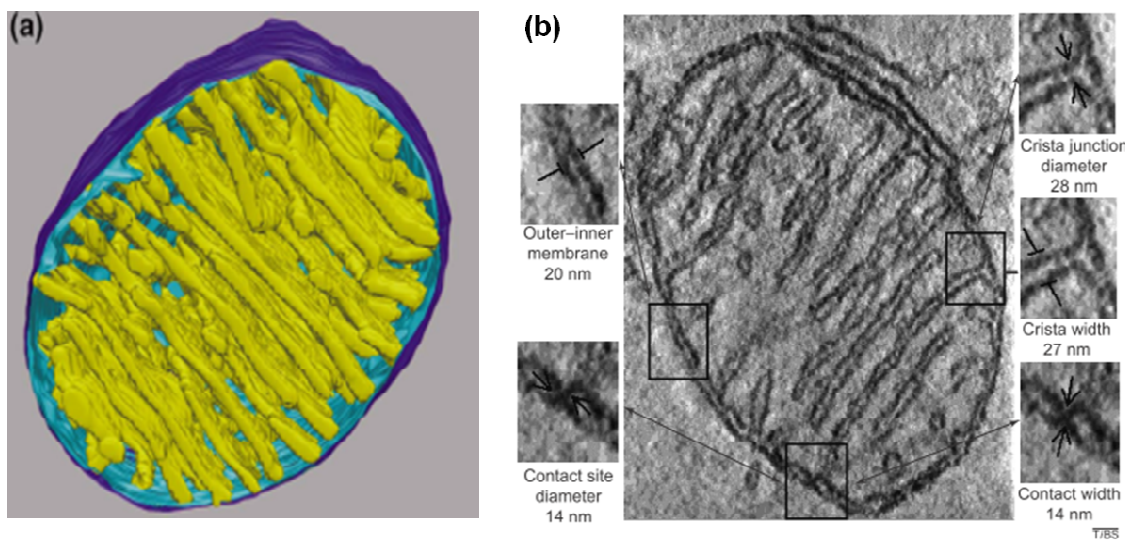


Figure 1. Mitochondria ultrastructure. (a) Computer model of mitochondrion section of chick cerebellum from segmented 3D tomograms. Model shows all cristae in yellow, the inner membrane boundary in light blue and the outer membrane in dark blue. (b) A single section through 3D tomogram of the mitochondrion used to create model in (a). From Frey and Mannella, 2000.

Mitochondrion matrix activity: β -oxidation and tricarboxylic acid cycle

Two of the most important metabolic pathways take place in the mitochondrial matrix. Glucose, fatty acids and amino acids are the three substrates that an organism can use to maintain energy homeostasis, not only for energy production but also for (macro)molecules biosynthesis. In particular, when glucose supply becomes limited (during fasting, for example), fatty acid degradation assumes a fundamental importance for the most of tissues. After a first hydrolysis by endothelium-bound lipases, the uptake by plasmatic membrane proteins and the conversion to acyl-CoAs, the further step of the fatty acids catabolism is the mitochondrial fatty acids β -oxidation (FAO). The mitochondrial membrane is impermeable to acyl-CoAs; for this reason, acyl-CoAs use the carnitine shuttle (CPT) for their import into mitochondria (Fig.2). CPT1 converts an acyl-CoA in acylcarnitine, which is translocated across the mitochondrial membrane by carnitine acylcarnitine translocase (CACT), exchanging a free carnitine molecule from the inside. CPT2, located at the inner membrane, reconverts acylcarnitines into their CoA esters, which can undergo FAO (van der Leij et al., 2000; Ramsay et al., 2001; Bonnefont et al., 2004). Once inside the mitochondria, acyl-CoAs are cleaved into acetyl-CoA units via the classic series of the four enzyme reactions called β -oxidation (Fig.2). The pathway is a cyclic process in which acyl-CoAs are shortened, whereby the two carboxy-terminal carbon atoms are released as acetyl-CoA units each time a cycle is fully completed. First, an acyl-CoA-ester is dehydrogenated to yield a trans-2-enoyl-CoA. This is followed by hydration of the double bond and in the third step the resulting L-3-hydroxy-acyl-CoA is dehydrogenated to 3-keto-acyl-CoA. Finally, thiolitic cleavage of the 3-keto-acyl-CoA produces a two-carbon chain-shortened acyl-CoA plus acetyl-CoA. Each cycle yields an acyl-CoA shortened by two carbon atoms, an acetyl-CoA, and one nicotinamide adenine dinucleotide (NADH) and one flavin adenine dinucleotide (FADH₂) as electron carriers (or reducing equivalents). The resulting acyl-CoAs enters another cycle of FAO whereas the electron carriers deliver the electrons to the electron transport chain and the acetyl-CoA can enter the tricarboxylic acids (TCA) cycle, also known as the citric acid cycle or the Krebs cycle (Krebs and Johnson, 1937). Indeed, the conversion of reducing power provided by carboxylic acids into the respiratory chain-usable reduced coenzymes NADH and FADH₂ constitutes a main function of TCA cycle. The TCA also plays a central role in an endless series of

metabolic pathways, in particular thanks to transamination reactions; moreover, several major anaplerotic pathways require the TCA cycle breakdown of acetyl-CoA and the multistep interconversion of carbon skeletons.

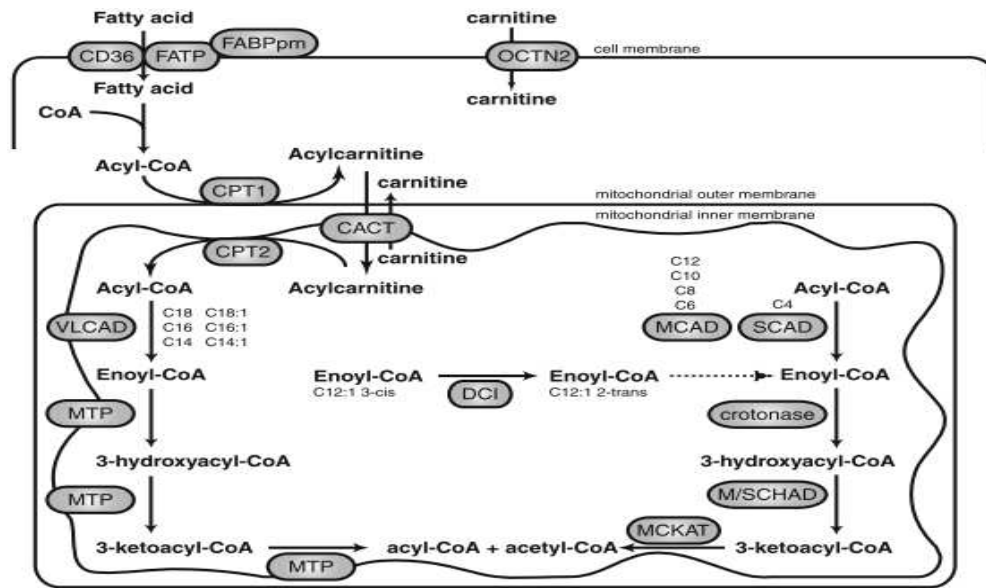


Figure 2. Mitochondrial β -oxidation in human. After transport across the plasma membrane, fatty acids are activated to acyl-CoAs at the cytosolic site. CPT1 converts the acyl-CoA into an acylcarnitine, which is subsequently transported across the mitochondrial membrane by CACT. CPT2 converts the acylcarnitine back into an acyl-CoA. Long chain acyl-CoAs are metabolised by the membrane bound enzymes, very long chain acyl-CoA dehydrogenase (VLCAD) and mitochondrial trifunctional protein (MTP), which has hydratase, long chain hydroxyacyl-CoA dehydrogenase (LCHAD) and thiolase activity. Short and medium chain acyl-CoAs are metabolised in the mitochondrial matrix by medium chain acyl-CoA dehydrogenase (MCAD), short chain acyl-CoA dehydrogenase (SCAD), crotonase, medium and short chain hydroxyacyl-CoA dehydrogenase (M/SCHAD) and medium chain 3-ketoacyl-CoA thiolase (MCKAT). The oxidation of unsaturated fatty acids such as oleic acid requires the action of an isomerase [dodecenoyl-CoA delta isomerase (DCI)]. C18 denotes an acyl-CoA with a chain length of 18 carbon atoms, and so forth. From Houten and Wanders, 2010.

More important, it is also the third step in carbohydrate catabolism, after conversion of glycolysis-produced pyruvate in acetyl-CoA, and the following step in protein catabolism after cleavage of amino acids and conversion in acetyl-CoA. The TCA cycle, that comprises eight reactions resulting in the progressive oxidative decarboxylation of acetyl CoA (Fig. 3), begins with the transfer of two-carbon acetyl group from acetyl-CoA to the four-carbon acceptor compound (oxaloacetate) to form the six-carbon compound citrate. The citrate then enters into a series of chemical transformations, losing two carboxylic groups as CO_2 ; most of energy made available by the oxidative steps is transferred to other metabolic process by GTP (or ATP) or as energy-rich electrons to NAD^+ generating NADH (for each acetyl group that enter in the TCA cycle, three molecules of NADH are produced) and to FADH to generate FADH_2 . The generated NADH may later on donate its electrons to the respiratory chain complex to drive ATP synthesis, whereas FADH_2 is covalently attached to succinate dehydrogenase, an enzyme functioning both in the TCA and the mitochondrial electron transport chain. FADH_2 , therefore, facilitates electrons transfer to coenzyme Q, which is the final acceptor of the reaction catalyzed by the succinate ubiquinone oxidoreductase complex, also acting as an intermediate in the electron transport chain. At the end of each TCA cycle, the four-carbon oxaloacetate has been regenerated to continue the cycle.

The mitochondrial membrane oxidative phosphorylation

The mitochondrial IM hosts the five protein complexes of oxidative phosphorylation (OXPHOS): complex I (NADH dehydrogenase or NADH:ubiquinone oxidoreductase), complex II (succinate dehydrogenase or succinate:ubiquinone oxidoreductase), complex III (the bc₁ complex or ubiquinone:cytochrome c oxidoreductase), complex IV (cytochrome c oxidase, cyclooxygenase or reduced cytochrome c: oxygen oxidoreductase) and complex V (ATP synthase). Additionally, OXPHOS system also involves two electron transport carriers: ubiquinone or coenzyme Q10 and cytochrome c. The electron transport chain is coupled to the generation of a proton gradient across the inner mitochondrial membrane, which is further used by the fifth enzymatic complex (F₀F₁-ATP synthase), to synthesize ATP from ADP and inorganic phosphate (Saraste, 1999) (Fig. 4).

Complex I (NADH dehydrogenase) is the largest of the respiratory complexes, comprising forty-five subunits, of which seven are mitochondrially encoded (Carroll et al., 2002). The enzyme contains multiple prosthetic groups, one flavomononucleotide (FMN) and eight iron-sulphur clusters (Carroll et al., 2006). Complex I transfers electrons from NADH to ubiquinone (CoQ), generating ubiquinol (CoQH₂), with the translocation of four protons across the inner membrane into the intermembrane space (Nicholls and Ferguson, 2002). Ubiquinol is also produced by complex II (succinate dehydrogenase), which oxidases succinate to fumarate in the Krebs cycle, and donates electrons to the respiratory chain, as written above. Complex II is the only respiratory enzyme completely encoded by the nucleus (Rustin et al., 2002), comprising a catalytic subunit, succinate dehydrogenase, and two membrane subunits, anchoring the complex into the mitochondrial IM (Capaldi et al., 1977). Electrons from succinate are donated to the covalently bound FAD of succinate dehydrogenase, reducing it to FADH₂. The electrons are further transported via a number of iron/sulphur clusters to CoQ, reducing it to CoQH₂ (Lancaster and Kroger, 2000; Saraste, 1999). A third source transferring electrons to generate ubiquinol is the glycerol-3-phosphate dehydrogenase enzyme.

Ubiquinol donates its two electrons consecutively to complex III (ubiquinol cytochrome c oxidoreductase) (Walker et al., 1992). One electron is transferred to cytochrome c via the Rieske iron-sulphur protein, while the second is transferred back to the matrix side, to cytochrome b of complex III. Cytochrome b is able to accept two electrons, which, in

turn, are donated to ubiquinone at the matrix side, generating ubiquinol. Due to the recycling of ubiquinone this process is also termed the Q-cycle (Darrouzet et al., 2001).

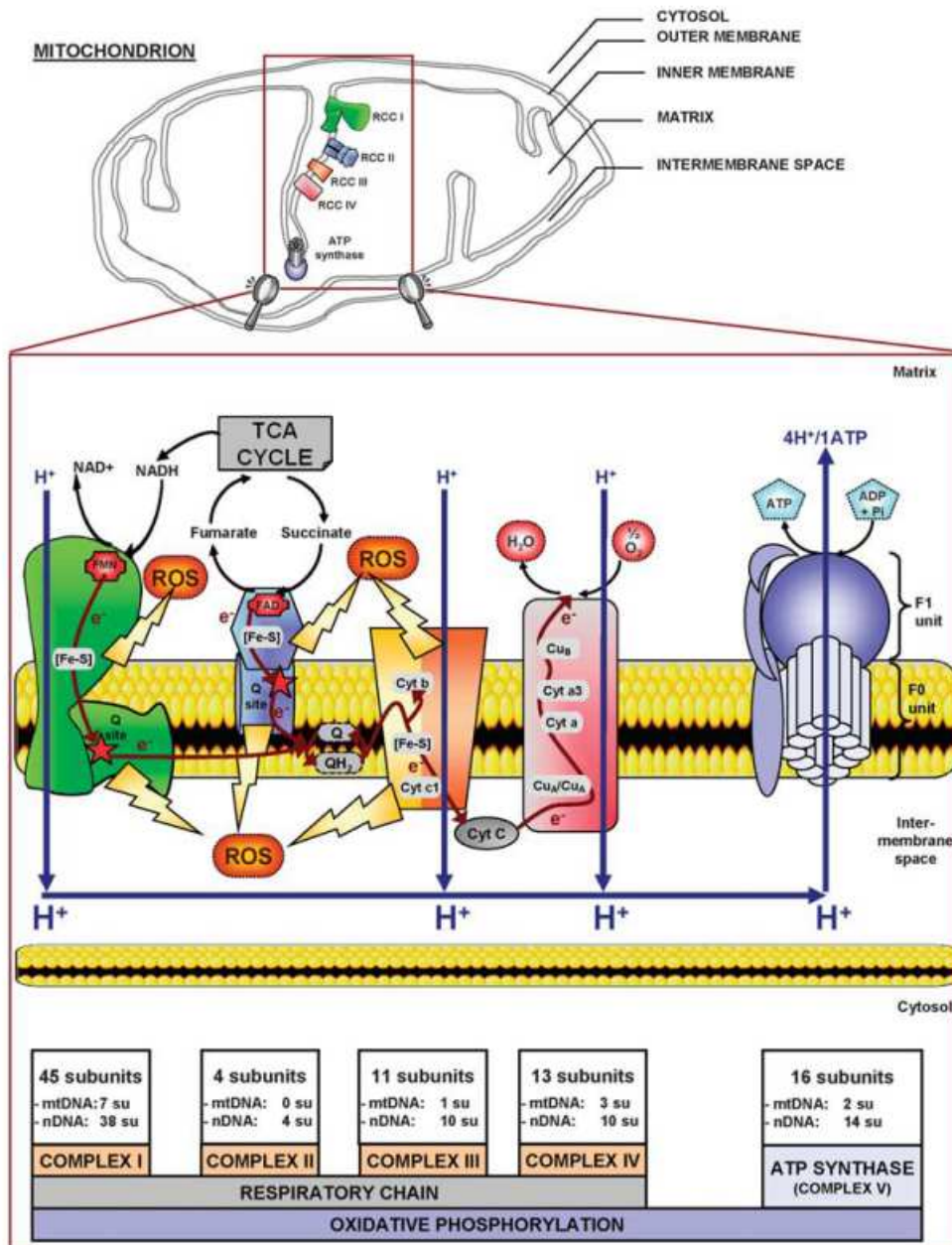


Figure 4. Representation of the mitochondrial respiratory chain complexes and the oxidative phosphorylation system. The four complexes of the respiratory chain and the ATP synthase are schematized and the electron/proton pathways along these complexes are indicated. From Lemarie and Grimm, 2011.

Complex III, the middle segment of the respiratory chain, transfers two electrons from CoQH₂ to cytochrome c, which then shuttles the electrons to complex IV (cytochrome c oxidase). Complex III couples electron transfer to the translocation of two protons across the IM. This complex has only one mtDNA-encoded subunit, cytochrome b; the other 10 subunits are nucleous-encoded, and at least one of these has been reported to be essential for the complex assembly (Berry et al., 2000; Yu et al., 1998; Zeviani et al., 2003). Cytochrome c is a water-soluble protein that donates electrons on the cytoplasmic side of the mitochondrial IM to complex IV. This is the terminal component of the respiratory chain, composed of 13 subunits, of which three are encoded by the mtDNA. Complex IV catalyzes the transfer of electrons from the reduced cytochrome c pool to molecular oxygen, reducing it to water. In this step, four electrons have to be donated from complex IV to two molecules of oxygen, without generating any reactive oxygen species. This is achieved by complex IV storing the four electrons on haem and copper atoms, before releasing them only in the presence of two molecules of oxygen and four protons at the matrix side of the mitochondrial IM. During this reaction four protons are translocated across the mitochondrial IM from the matrix side to the intermembrane space (Schultz and Chan, 2001).

The energy released by the flow of electrons through the respiratory chain is used to pump protons through the mitochondrial inner membrane by complexes I, III, and IV. This electrochemical gradient is finally utilized by the ATP synthase (F₁ F₀ -ATPase) to generate ATP (Saraste, 1999). This complex is bipartite, as implied by the nomenclature, composed of a membrane-bound portion (F₀) and a large extra-membranous portion (F₁) that protrudes into the matrix space. F₁ and F₀ are linked together by two stalks (Capaldi and Aggeker, 2002). Complex V has two subunits encoded by mtDNA (ATPase6 and ATPase8), that take part to the membrane-bound portion (F₀) of the complex, and about 13 other subunits encoded by nDNA (Abrahams et al., 1994). Protons from the intermembrane space enter complex V through the F₀ complex leading to subunit rotation within the complex. The energy from this rotation is then used for ATP synthesis, which takes place in the F₁ complex (Schultz and Chan, 2001). The ATP synthesized in the mitochondrial matrix is transported across the inner mitochondrial membrane in exchange with cytosolic ADP, through the adenine

nucleotide translocator (ANT), an energetically favourable reaction driven by the voltage gradient across the IM (Saraste, 1999).

The knowledge about the overall organization of the five respiratory complexes is changed in the last decade. In fact, a fluid-state model, based on the idea that complexes are freely diffuse in the IM and that electron transfer is based on random collision of single complexes, has been replaced by a solid-state model, which propose a stable interaction between OXPHOS complexes within entities named supercomplexes. This model is now supported by a wide range of experimental findings that demonstrated a strict association between the respiratory complexes in mitochondria of yeast, plants and mammals (Schagger and Pfeiffer 2000; Krause et al, 2004; Schafer et al., 2006). The supramolecular organization of the OXPHOS system is considered to be of great functional importance. Formation of supercomplexes plays a role in the assembly and stability of the complexes, suggesting that the supercomplexes are the functional state of the respiratory chain (Vonck et al., 2009). Respiratory supercomplexes may (i) allow enhanced electron transfer rates by electron channeling, (ii) represent regulatory units of respiration, (iii) determine the ultrastructure of the inner mitochondrial membrane, (iv) increase the stability of OXPHOS complexes, and (v) increase the protein insertion capacity of the mitochondrial IM. Several experimental observations confirm one or the other roles of the OXPHOS supercomplexes (Boekema et al., 2007).

Mitochondrial DNA

Mitochondria contain the only extranuclear source of DNA in animal cells (Nass, 1966). MtDNA is a circular, double-stranded, 16569 base pair molecule of DNA which encodes 37 genes, including 13 essential polypeptides for the OXPHOS system, 2 ribosomal RNAs (12S and 16S) and 22 tRNAs (Anderson et al, 1981) (Fig. 5). The remaining proteins required for mitochondrial metabolism and maintenance are synthesized in the cytosol and are specifically targeted, sorted and imported to their correct mitochondrial location (Mokranjac and Neupert, 2005). The mitochondrial genome has unique characteristics which distinguish it from the nuclear genome; it is strictly maternally inherited and there are several hundred to several thousand of copies

within a single cell. The number of copies present varies between different cell types depending on the energy demand within the tissue (Taylor and Turnbull, 2005). There are no introns and the genes have either none, or very few non-coding bases between them and in most cases termination codons are not present, but are created post-transcriptionally by polyadenylation (Anderson et al., 1981). There are only two non-coding regions in the mtDNA and they contain most of the known regulatory functions. The major one is the 1 kb displacement D-loop, characterized by the presence of a triple strand structure, due to association of the new H-strand in this region (Fernandez-Silva et al., 2003). The D-loop contains the origin of H-strand DNA replication (OH) and is also the site of transcription from opposing heavy and light strand promoters (Clayton, 2000; Scarpulla, 2008). The second non-coding region is about 30 nucleotides long and contains the origin of L-strand replication (OL). This region is located in a cluster of five tRNA genes around two thirds of the mtDNA length from the OH (Anderson et al., 1981; Fernandez-Silva et al., 2003).

The physiological polyploidy of the mitochondrial genome gives rise to a peculiar genetic inheritance which is dominated by the phenomena of homo- and heteroplasmy, the latter being the coexistence in one cell of two or even more different mitochondrial genotypes. It is generally accepted that as mutations may arise in one copy of the mtDNA, they may hence be selected against or shift to increase the mutation load within a cell until detrimental effects take over or a pathological phenotype sets in. This threshold level may vary according to the mutation type; it has been shown in neurodegenerative diseases that the penetrance or the severity of a condition may well depend on the heteroplasmy level in the individual (Carelli et al., 2002; Laloi-Michelin et al., 2009); it has also been demonstrated that the tumorigenic potential associated to a particular mitochondrial mutation reveals itself only at a exact mutation load (Gasparre et al, 2011; Park et al., 2009).

MtDNA shows a higher mutation rate than nuclear DNA (Nachman et al., 1996; Schriener et al., 2000) and that is due to a number of elements, among which (i) the proximity to reactive oxygen species production sites, (ii) the lack of protective histones, (iii) the highly compact structure which lacks buffering sequences such as introns and (iv) a less efficient DNA repairing system.

Another particular feature of mtDNA is the strict maternal inheritance: mtDNAs can only evolve by the sequential accumulation of mutations along radiating maternal lineages. For this reason, if an mtDNA mutation arises that is beneficial in a particular environment, it and its descendants will increase in frequency in that environment. This results in the generation of a group of related mtDNA haplotypes (haplogroups) concentrated in a particular geographical region. The human mtDNA sequence is highly variable, and approximately one-fourth to one-third of mtDNA polypeptide and structural RNA sequence variants appear to be functionally important; natural selection then enriches for the regionally appropriate coupling efficiency and thus mtDNA haplogroup (Mishmar et al., 2003; Wallace et al., 2003; Ruiz-Pesini et al., 2004; Ruiz-Pesini and Wallace, 2006).

MITOCHONDRIAL DISEASES

Mitochondrial diseases can be caused by mutations in mitochondrial DNA and by mutations in nuclear DNA.

MtDNA mutations causing diseases were first reported in 1988 (Wallace et al., 1988; Holt et al., 1988) and since then more than 300 pathogenic mtDNA mutations have been described. MtDNA genetics is very complex because mutations in different mitochondrial genes can give similar phenotypes, mutations in the same gene can give different phenotypes, and the same mtDNA mutation at different levels of heteroplasmy can result in very different phenotypes.

Clinically relevant mtDNA variants fall into three classes: (i) recent deleterious mutations resulting in maternally transmitted disease, (ii) ancient adaptive variants that predispose individuals to disease in different environments, and (iii) the age-related accumulation of somatic mtDNA mutations that erode function and provide the aging clock (Wallace, 2005). Diseases due to rearrangement mutations and base substitution mutations belong to the first class and they include: maternally inherited Type II diabetes; deafness chronic progressive external ophthalmoplegia (CPEO), Kearns–Sayre syndrome (KSS) associated with ophthalmoplegia, ptosis, and mitochondrial myopathy with ragged red fibers (RRFs) (Mita et al., 1989; Wallace et al., 2001; Wallace and Lott, 2002; Wallace, 2005); the Pearson marrow/pancreas syndrome (Kapsa et al., 1994); LHON (Wallace et al., 1988); Leigh syndrome (Holt et al., 1990); mitochondrial myopathy (Andreu et al., 1998, 1999a,b); MERRF (Wallace et al., 1988b; Shoffner et al., 1990); MELAS (Goto et al., 1990); encephalomyopathy; Alzheimer’s disease (AD) and Parkinson’s disease (PD) (Shoffner et al., 1993; Khusnutdinova et al., 2008). The second class (ii) of variants depends on the ancient adaptive haplogroups which still influence individual predisposition to a wide spectrum of common diseases today. To make some examples, the first evidence that mtDNA haplogroups could modify disease predisposition was the discovery that European haplogroup J increases penetrance of the milder LHON mutations (Brown et al., 1995, 1997, 2002; Torroni et al., 1997; Ghelli et al., 2009). On the other hand, it has also been demonstrated that haplogroup J correlates also with longevity in Europeans (Ivanova et al., 1998; De Benedictis et al., 1999; Rose et al., 2001) but also with a more rapid AIDS progression (Hendrickson et al., 2008). In

addition, mtDNA haplogroups have also been correlated with athletic performance, which is consistent with different mtDNA haplogroups having different mitochondrial ATP production competence, due to differential coupling efficiency (Scott et al., 2005, 2009).

About the third variant class (iii), mutations in the mtDNA have been observed to accumulate with age in a variety of postmitotic tissues in a wide range of species and in a spectrum of complex age-related diseases (Wallace, 2005c). Increasing the mtDNA mutation rate in mice increases their aging rate (Trifunovic et al., 2004; Kujoth et al., 2005), while decreasing the somatic mtDNA mutation rate by introducing catalase into the mitochondrial matrix extends mouse life span (Schriner et al., 2005). Therefore, the accumulation of somatic mtDNA mutations provides an aging clock that helps defining an animal's life span and contributes to the delayed-onset and progressive course of complex diseases (Wallace, 2005c). Cancer is also (but not only) an age-related disease, and both somatic and germline mtDNA mutations have been reported in cancers including renal adenocarcinoma, colon cancer cells, head and neck tumors, astrocytic tumors, thyroid tumors, breast tumors, prostate tumors, etc. (Wallace, 2005a; Brandon et al., 2006) (see "Mitochondrial metabolic dysfunction and cancer" paragraph). Besides, mitochondrial ROS production appears to be an important component of carcinogenesis (Petros et al., 2005; Ishikawa et al., 2008).

Mutations in nDNA-encoded OXPHOS genes have also been linked to a variety of multisystem disorders ranging from lethal childhood Leigh syndrome to predisposition to depression. Mutations in the structural subunits of Complexes I and II and in a Complex IV assembly factor, SURF1 (Zhu et al., 1998; Procaccio and Wallace, 2004), can cause severe OXPHOS defects and result in the lethal childhood disease, Leigh syndrome. Mutations in the nDNA POLG or Twinkle helicase are associated with multiple mtDNA deletions and have been linked to autosomal dominant or autosomal recessive progressive external ophthalmoplegia (PEO). POLG mutations can cause a broad spectrum of diseases from mild myopathy to lethal Alpers syndrome (Spelbrink et al., 2001; Van Goethem et al., 2001). Some ANT1 gene mutations can inactivate the protein and result in autosomal recessive myopathy and cardiomyopathy associated with multiple mtDNA deletions without PEO (Palmieri et al., 2005). However, other ANT1 missense mutations act as dominants and cause autosomal dominant PEO, associated

with the accumulation of multiple mtDNA deletions (Kaukonen et al., 2000). Mutations in deoxyguanosine kinase and mitochondrial thymidine kinase 2 cause mtDNA depletion (Mandel et al., 2001; Saada et al., 2001), and mutations in succinyl-CoA synthase subunit SUCLA2 cause mild methylmalonic aciduria, Leigh-like encephalomyopathy, dystonia, and deafness in association with mtDNA depletion (Carrozzo et al., 2007). Mutations in the cytosolic thymidine phosphorylase cause mitochondrial neurogastrointestinal encephalomyopathy (Nishino et al., 1999) associated with mtDNA deletions and depletion. Mutations in the gene encoding the mitochondrial fusion protein OPA1 cause autosomal dominant optic atrophy (Delettre et al., 2000), while mutations in mitofusin2 result in the peripheral neuropathy, Charcot-Marie-Tooth 2 (Zuchner et al., 2004). Mitochondrial diseases can also result from defects in the genes for mitochondrial metabolic proteins. For example, defects in coenzyme Q10 metabolism and various Krebs cycle enzyme genes have been reported (Wallace et al., 2007b, 2010).

MITOCHONDRIAL METABOLIC DYSFUNCTION AND CANCER

Defects in mitochondrial function have long been suspected to contribute to the development and possibly progression of cancer: in 1930, Otto Warburg proposed that cancer was caused by defects in OXPHOS or respiration in the mitochondria, forcing cells to shift to energy generation process through glycolysis, despite aerobic conditions. After several decades of research related to what is defined “Warburg effect” in tumor, during the past few years it is being reconsidered but it continues to be a subject of even more increasing interest in cancer research. In fact, it is becoming clear that it plays an important role in tumor development by remodeling the metabolic profile of tumor cells, which allows cell survival under adverse conditions. Since the description of the Warburg effect, several studies have shown that cancer cell mitochondria are small, possess few cristae, have a characteristic shape and size and an altered membrane, but only in last decade mutations in gene encoding mitochondrial proteins were demonstrated to be directly involved in tumorigenesis. Like in the neurodegenerative diseases, both nDNA and mtDNA mutations have been found implicated in human cancer. In particular, three mitochondrial enzymatic functions, between TCA and OXPHOS, are affected by nuclear gene mutations and are involved in tumorigenesis process of different tumors.

Nuclear genes involved in mitochondrial defects in cancer

Mitochondrial succinate-coenzyme Q oxidoreductase or complex II of the respiratory chain catalyzes the conversion of succinate to fumarate in the TCA cycle and simultaneously transfers electrons from succinate to coenzyme Q. It is comprised of four nuclear-encoded subunits, SDHA, SDHB, SDHC and SDHD (Fig. 6), whose both germinal and somatic loss-of-function mutations have been described and appreciated in paragangliomas (PCC), in renal cell carcinomas (RCC) and in pancreatic cell cancers (PCC) (Baysal et al. 2000; Housley et al., 2010; Ricketts et al., 2008; van Nederveen et al., 2007). It was also found that mutations in SDHC, SDHB and SDHD are correlated with the rare development of a combination of hPGL and GIST (gastrointestinal stromal

tumor), defined as Carney-Stratakis syndrome, and with the non-familial Carney triad, characterized by the presence of extra-adrenal paragangliomas, GIST and pulmonary chondromas (Stratakis and Carney, 2009).

Loss-of-function germline mutations in another TCA nuclear-encoded enzyme, fumarate hydratase (FH), which catalyzes the reversible conversion of fumarate to malate, predispose to hereditary leiomyomatosis and renal cell cancer (HLRCC), inherited leiomyomas (generally benign tumors of the smooth muscle), and renal (type II papillary and collecting duct) carcinoma (Launonen et al., 2001; Tomlinson et al., 2002). There is evidence suggesting that FH mutations may also be involved in the pathogenesis of breast, bladder, and testicular (Leydig cell) cancers (Carvajal-Carmona et al., 2006; Lehtonen et al., 2006). Similar to SDH in hPGL, enzymatic activity of FH is absent in HLRCC tumors and loss of the wild-type allele is observed in the majority of tumors (Tomlinson et al., 2002).

Somatic mutations in isocitrate dehydrogenase (IDH), which catalyzes the oxidative decarboxylation of isocitrate to α -ketoglutarate in TCA cycle, have been identified in gliomas and acute myelogenous leukemia (AML) (Carroll et al., 2010; Parsons et al., 2008; Bleeker et al., 2009; Yan et al., 2009). While FH and SDH mutations are typically loss-of-function, and for this reason their genes believed tumor suppressors, some IDH mutations lead to a gain of a new NADPH-dependent α -ketoglutarate-reductase activity with production of a less known metabolite, 2-hydroxyglutarate (2HG), significantly accumulated in glioma cells and blood of AML patients and defined “oncometabolite”, to portray its potential oncogenic contribution (Dang et al., 2009; Frezza et al., 2010).

In all these three genetic-metabolic events, the underlying mechanism of tumorigenesis involves the accumulation of metabolites that convey oncogenic signal. Even though the role of 2HG is still unclear, succinate and fumarate accumulation, observed in the tumors with mutations in SDH and FH respectively, has been linked to the tumoral progression by hypoxia inducible factor (HIF) activation. HIF is known to orchestrate the metabolic and genetic reprogramming required to sustain tumor cell growth, vascularization and proliferation. The molecular link between TCA dysfunction and HIF activation was initially proposed by Selak and co-workers (Selak et al. 2005), but subsequently followed and proved by several other research groups (Gottlieb and Tomlinson, 2005; Isaacs et al., 2005; Pollard et al., 2005; Hewitson et al., 2007; Porcelli

et al., 2010). In summary, in normoxic condition, HIF1 α prolyl 4-hydroxylase, master regulator of HIF stability, hydroxylates two proline residues on the oxygen-dependent degradation domain of HIF1 α , targeting it to the ubiquitin-proteasome degradation machinery. This hydroxylation requires oxygen and α -ketoglutarate and produce carbon dioxide and succinate. For this reason, the succinate accumulation in SDH-deficient cell tumors impairs PHDs activity and leads to HIF1 α stabilization also under normoxic conditions, a phenomenon that has been defined as pseudohypoxia (Gottlieb and Tomlinson, 2005). Also fumarate has been demonstrated to be a potent inhibitor of PDHs (Isaacs et al., 2005). Furthermore, other biochemical studies showed that PHD activity is competitively inhibited by succinate or fumarate and, therefore, the ratio between α -ketoglutarate and succinate (or fumarate) rather than the absolute concentrations of these metabolites dictates PHD activity (MacKenzie et al., 2007; Porcelli et al., 2010). However, the activity of other enzymes could be affected by the TCA cycle intermediates accumulation like the α -ketoglutarate-dependent dioxygenases (Schofield and Ratcliffe, 2004) or the histone demethylase JMJD3 (Cervera et al., 2009), carrying to speculate about the mitochondria to-cytosol and mitochondria to-nucleus signalings of succinate and fumarate, with the power to regulate gene expression.

In addition, somatic and germinal mutations in NDUFA13, subunit of respiratory complex I, are linked to Hürthle cell tumors of the thyroid (Maximo et al., 2008), and its down-regulation or loss of its expression has been reported in renal cell carcinomas (RCC) and colorectal carcinoma (Maximo et al., 2008; Gong et al., 2007; Kalakonda et al., 2007).

Then, mutations in gene of the polymerase-gamma (POLG) gene, the only DNA polymerase known to function in human mitochondria, was mutated in 63% of breast tumors (Singh et al., 2009a; Chan and Copeland, 2009; Wong et al., 2008) inducing a depletion of mtDNA, decreased mitochondrial activity, decreased mitochondrial membrane potential, increased levels of reactive oxygen species and increased matrigel invasion (Singh et al. 2009a,b).

Altogether, these findings suggest a role for OXPHOS dysfunction in cancers and in promoting tumorigenicity.

Mitochondrial genes involved in defective OXPHOS in cancer

Mitochondrial DNA mutations have been increasingly identified in various types of cancer (Polyak et al., 1998; Fliss et al., 2000). A number of mtDNA rearrangements and amplifications have been reported in acute myeloid leukemia (Boulton et al., 1996) and point mutations in human colorectal cancer cells (Polyak et al., 1998), esophageal, ovarian, thyroid, head, neck, lung, bladder, renal, and breast cancer cells (Fliss et al., 2000; Brandon et al., 2006; Chatterjee et al., 2006; Shidara et al., 2005).

Mutations in mtDNA have been described in tRNAs, rRNA, protein encoding regions, and important feature, in D-loop region, the single control region of mtDNA for replication and transcription of its OXPHOS genes. Mutations in the D-loop region result in altered binding affinities of the nuclear proteins involved in mtDNA replication and transcription leading to the depletion of mtDNA content (Clayton, 2000). Decreased mtDNA level has been reported in breast (Tseng et al., 2006), renal (Selvanayagam and Rajaraman, 1996), hepatocellular (Lee et al., 2005; Yin et al., 2004), gastric (Wu et al., 2005), liver (Yin et al., 2004), and prostate tumors (Moro et al., 2008). Depletion of mtDNA is also supported by a decrease in OXPHOS levels in renal tumors (Simonnet et al., 2002). Therefore, it has been demonstrated that reduced mtDNA leads to increased invasiveness and aggressive disease (Simonnet et al., 2002; Mambo et al., 2005).

Since the mitochondrial mutations affect the synthesis of peptides that are important components of various respiratory chain complexes, the ultimate outcome is likely to be defective OXPHOS. MtDNA-derived subunits of respiratory chain complex I (7/45 subunits: NADH dehydrogenase subunits ND1 to ND6 and ND4L), III (1/11 subunits: cytochrome b) and IV (3/13 subunits, cytochrome c oxidase subunits COXI to III) have been found altered in various types of cancers (Brandon et al., 2006; Lu et al., 2009) (Fig. 6).

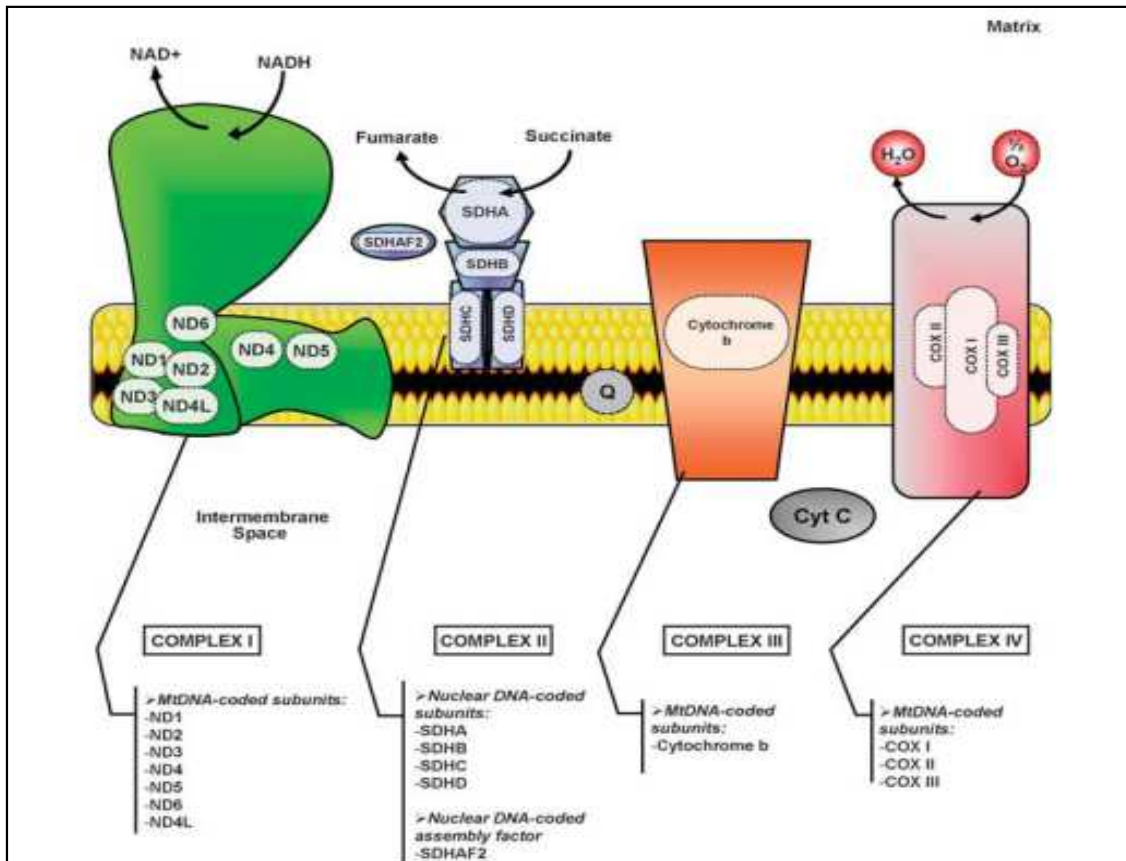


Figure 6. The four complexes of the respiratory chain are schematized and the various mutations found in cancer cells that impact complex subunits and assembly factors are highlighted: ND1-6 and ND4L (nicotinamide adenine dinucleotide, NADH, dehydrogenase subunits 1–6 and 4L); SDHA–D (succinate dehydrogenase subunits A–D), SDHAF2 (SDH assembly factor 2); cytochrome b; COXI–III (cytochrome c oxidase subunits I–III). From Lemarie and Grimm, 2011.

An important question was if these mutations act as a significant cause of tumourigenesis or if they merely constitute a side effect of tumour development. Only recently different groups have supported the likelihood of a causative effect on tumour progression. In thyroid cancer cell lines (Abu-Amero et al., 2005), renal (Gasparre et al., 2008) and thyroid oncocytomas (Gasparre et al., 2007) for example, mtDNA mutations in the complex I subunits ND1, ND2 and ND4–6 were shown to be associated with complex I deficiency and enhanced proliferation. Therefore, human cells bearing a ND5 mutation were associated with a drop in oxygen consumption, increased ROS production, potentiated glucose dependency and enhanced tumour growth (Park et al., 2009). MtDNA mutations of the complex IV subunit COXI were found in 11 to 12% of all prostate cancer patients screened in one study and associated with a complete loss of the COXI protein in tumoral tissues and an increased tumour growth rate (Petros et al., 2005). It was shown that mutations in mtDNA of complex I (ND1) and III (cytochrome b) led to a considerable decrease of both enzymatic activities and to ROS overproduction in thyroid carcinoma (Bonora et al., 2006). In accordance, another study established that the ND6 mutation confers a high metastatic potential to its transmitochondrial cybrid and was associated with a profound complex I deficiency and an overproduction of ROS (Ishikawa et al., 2008). The transmitochondrial cybrid cell model, in which mitochondria from tumour cells are transferred into cells devoid of their own mtDNA, allows to study mitochondrial mutations independently of their nuclear DNA. Another result obtained through a cybrid model for the relevance of mtDNA mutations in cancer progression, was provided by a mutant form of ATP6 (one of the two mtDNA-coded subunits of ATP synthase), that showed the positive contribution of the ATP6 mutant to tumour growth in mice through a decreased respiration rate, a higher proliferation in culture and a significant resistance to apoptosis (Shidara et al., 2005).

To summarize, it seems that mitochondrial mutations are linked to the tumoral progress by determining several effects, like (i) the decrease of one or more respiratory chain complex activities, (ii) an impaired electron flux along the respiratory chain associated with a reduced oxygen consumption, (iii) an increase in the electron leakage outside the affected respiratory chain leading to an increase of the basal ROS production and to the subsequent alterations of mtDNA, (iv) a global resistance to apoptotic processes

(Kwong et al., 2007) and finally (v) an enhanced proliferation and growth, instigating the development of tumour formation (Lu et al., 2009).

To conclude, it appears clear that, among the complex activities affected by both nuclear and even more mitochondrial mutations, complex I activity certainly holds a central position, having its subunits genes the highest mutational rate of mtDNA (Fig. 7): in particular, ND1 gene is indeed a hotspot for somatic changes with a ratio of over 3, meaning that mutations occur in this gene at a frequency more than three times higher than expected on the basis of the gene length. Our research group showed and explained the involvement and effects of a *MTND1* truncating mutation *in vivo* in oncocytic tumors and also in the only existing cell model of thyroid oncocytoma, demonstrating as the strong energetic impairment observed to be associated to this mutation was due to the complex I disassembly (Gasparre et al., 2007, 2008, 2010, 2011).

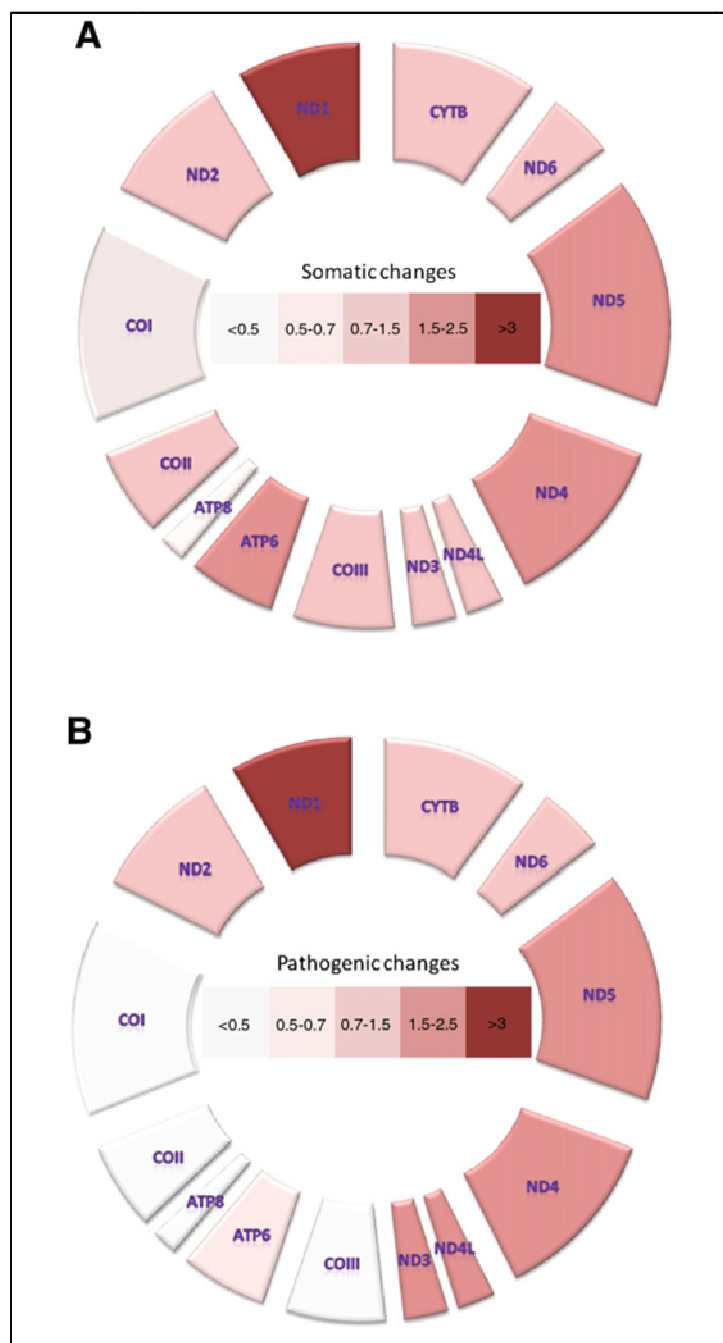


Figure 7. Frequency ratio of mtDNA mutations occurring in protein-coding genes. (A) Somatic changes. (B) Potentially pathogenic changes as predicted by PolyPhen. Different shades of colour indicate different susceptibility to mutations occurrence. Scale value from 0 to above 3 was calculated as ratio of mutation frequencies (obtained dividing the single values reported in Tab.1A and B per gene by the overall number of mutations) over the percentage of mtDNA occupied by the gene. Genes with values below 0.7 have been arbitrarily defined as “preserved from the occurrence of mutations”, whereas genes with values above 1.5 have been defined as “mutational hotspots”. From Gasparre et al., *Biochim Biophys Acta*.2011.

COMPLEX I : STRUCTURE, ASSEMBLY AND FUNCTION

Complex I, NADH:ubiquinone oxidoreductase, is the largest membrane protein assembly known and has a central role in energy production by the mitochondrial respiratory chain, providing about 40% of the proton-motive force required for the synthesis of ATP. Eukaryotic complex I is located in the mitochondrial inner membrane and protrudes into the matrix to form an L-shaped structure (Fig. 8). This structure consists of a hydrophilic peripheral arm with a hydrophobic membrane arm lying perpendicular to it (Friedrich and Bottcher, 2004). The L-shaped structure is conserved from NDH-1 in *Escherichia coli*, which is a homolog of eukaryotic complex I (Guenebaut V, et al., 1998; Sazanov LA et al., 2003), to bovine heart complex I (Friedrich and Bottcher, 2004). Over the years, extensive analyses of the intact complex and various subcomplexes from bovine heart mitochondria have played an important role in defining its subunit composition, especially by Walker and colleagues. In fact, they have resolved the intact complex I, with mildly chaotropic detergents, into four subcomplexes, I α , I β , I γ and I λ (Carroll et al., 2002, 2003; Sazanov et al 2000). Their separation has been carried out by three independent methods (1D SDS-PAGE, 2D IEF/SDS-PAGE, and reversed-phase HPLC) and subsequent analysis of the individual subunits has been done by mass fingerprinting and mass spectrometry (Carroll et al., 2003). Subcomplex I α consisted of the hydrophilic peripheral arm plus part of the hydrophobic membrane arm, as subcomplex I β contained the main part of the membrane arm. However, some subunits have not been found in either I α or I β and have been together considered as subcomplex I γ ; under slightly different conditions, I α dissociated to produce subcomplex I λ representing the hydrophilic or peripheral arm.

The further crystal structure defining of the hydrophilic domain of complex I in the bacterium *Thermus thermophilus* has allowed to make clear the relative positions of the 8 subunits that compose the peripheral arm of complex I (Sazanov et al., 2006). It consists of 2 functional modules, an electron input module (N module) and an electron output module (Q module), and comprises all redox active cofactors (Fig. 9). The N module contains an NADH oxidation site with an FMN molecule as the primary electron acceptor, while the Q module contains a ubiquinone reduction site. Electrons from the oxidation of NADH are transferred via FMN and a series of Fe–S clusters to

ubiquinone. The membrane arm or the proton translocation module (P module) contains the 3 subunits, ND2, ND4 and ND5. They are highly hydrophobic proteins, containing around 15 transmembrane stretches, and are antiporter-like subunits presumably involved in proton-pumping activity (Mathiesen et al., 2002). However, how electron transfer is coupled to proton translocation, either by direct association through protein binding sites or indirectly through conformational changes of the enzyme, remained obscure because of the lack of a high quality 3-dimensional structure of complex I (Belevich et al., 2006; Faxen et al., 2005).

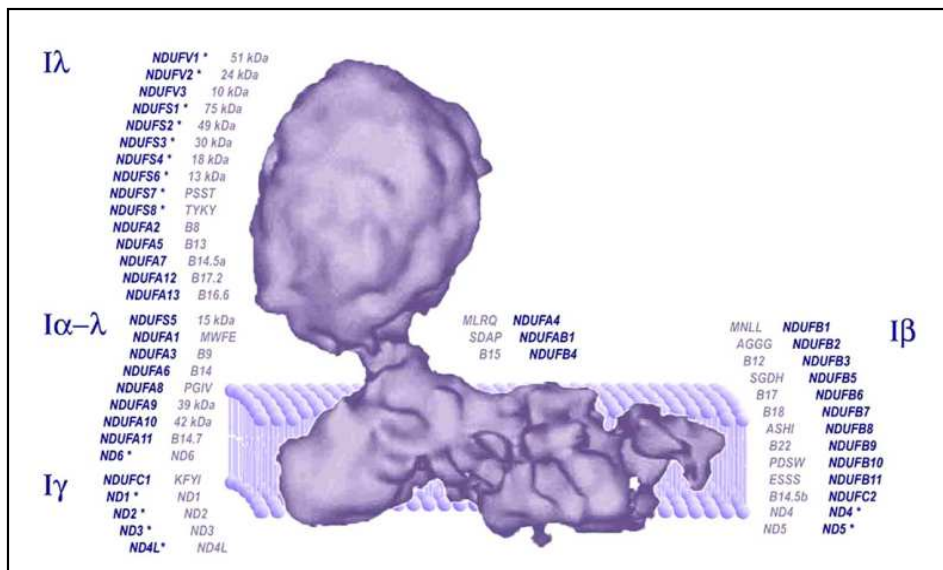


Figure 8. Subunit composition of mammalian complex I. Subunits have been grouped by the subcomplex they have been identified in, after complex I fractionation according to Walker and co-workers (Carroll et al., 2003). The human subunit nomenclature is shown in dark blue, the bovine one in light blue. Subunits depicted with a * have been reported harbouring pathogenic mutations causing complex I deficiency. From Janssen et al., 2006.

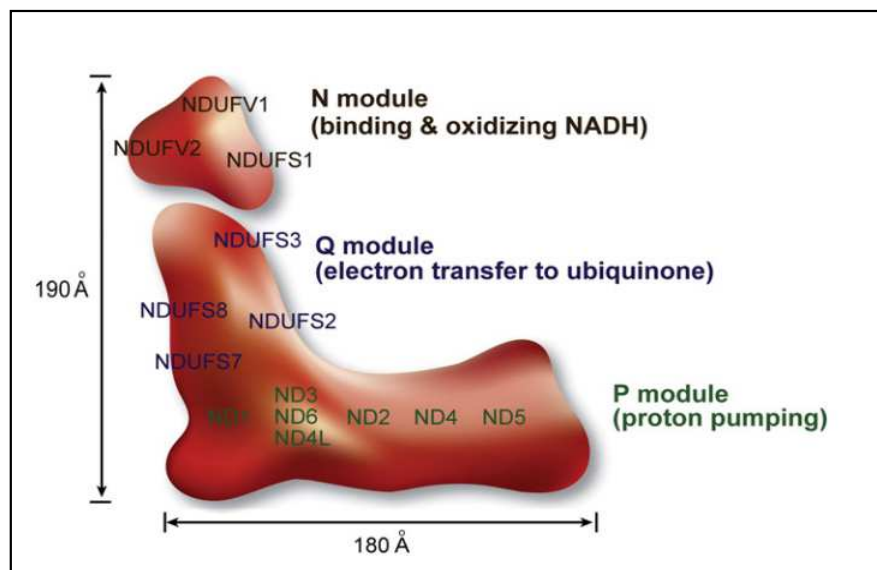


Figure 9. Schematic graph of functional structure of mammalian mitochondrial complex I. The matrix arm and the membrane arm form an L-shaped structure, with an angle of 100° . It is composed of three conserved functional modules: the NADH dehydrogenase module (N module), the electron transfer module (Q module) and the proton translocation module (P module). The positions of 14 core subunits are indicated, all of which are highly conserved from prokaryotes to eukaryotes. From Mimaki M et al., 2011.

More recently, the X-ray structures of the membrane domain of complex I from *E.coli* at a resolution of 3.9 \AA and of the entire complex I from *T. thermophilus* at a resolution of 4.5 \AA were solved (Efremov et al., 2010). These findings defined the positions of all of the subunits and revealed the long horizontal α -helical structure of the membrane domain of complex I, suggesting that the conformational changes at the interface of the matrix and membrane domains may drive the long amphipathic α -helices in a piston-like motion, thereby leading to proton translocation. In addition, the low resolution X-ray structure of mitochondrial complex I from the aerobic yeast *Yarrowia lipolytica* was also reported (Hunte et al., 2010). The arrangement of functional modules suggested the conformational coupling of redox chemistry with proton pumping. A long helical element in the NuoL/ND5 subunit stretches across the matrix face of the membrane domain of complex I and is suggested to be critical for transducing conformational energy to proton-pumping elements in the distal module of the membrane arm.

Bovine and human mitochondrial complex I consist of 45 different subunits, nuclear- and mitochondrial-DNA coded, with a total molecular weight of $\sim 980 \text{ kDa}$ (Carroll et

al., 2003, 2006). Generally, the NDU prefix (from NADH dehydrogenase ubiquinone) is used to distinguish the nuclear-encoded subunits from those mitochondrial-encoded ones, for which the ND prefix (from NADH dehydrogenase) is used. Seven subunits, ND1–ND6 and ND4L, are encoded by mitochondrial DNA, and are homologs of the 7 membrane subunits in bacterial NDH-1, forming the major part of the membrane domain (Janssen and al. 2006; Hirst et al. 2003). The mtDNA-encoded subunits are thought to be involved in proton translocation and ubiquinone binding (P module, Fig. 9), as their bacterial homologs have these functions (Janssen and al. 2006; Friedrich and Bottcher, 2004). The remaining 38 subunits are encoded by nuclear DNA and imported into the mitochondria (Hirst et al. 2003; Stojanovski et al., 2003; Hoogenraad et al., 2002). Seven of the nDNA-encoded subunits, NDUFV1, NDUFV2, NDUFS1, NDUFS2, NDUFS3, NDUFS7 and NDUFS8, represent the “core subunits” in the peripheral arm of complex I, catalyzing the oxidation of NADH and electron transfer (Janssen and al. 2006; Lazarou et al. 2009). The N module, responsible for the oxidation of NADH, includes at a minimum the NDUFV1, NDUFV2 and NDUFS1 subunits. The Q module, responsible for the electron transfer to ubiquinone, includes at a minimum the NDUFS2, NDUFS3, NDUFS7 and NDUFS8 subunits (Vogel et al., 2007) (Fig. 9). The remaining 31 nDNA-encoded subunits are referred to as “supernumerary” subunits because they have no counterparts in NDH-1 (Carroll et al., 2006). Most of the supernumerary subunits are not involved in enzymatic activity, and their actual function is still unknown. It has been proposed that the eukaryotic supernumerary subunits assist in the biogenesis of the complex and support its structural stability (Carroll et al., 2003, Friedrich and Bottcher, 2004).

The assembly of a so large protein complex was demonstrated to be a very complicated process, especially due to its dual genomic controls and to the numerous subunits. The nDNA-encoded subunits must assemble in coordination with the hydrophobic mtDNA-encoded subunits to form the properly functioning mature complex; however, the assembly pathway is still not completely understood. A number of model systems have been employed to study the assembly of the eukaryotic complex, in various organisms such as the green alga *Chlamydomonas reinhardtii*, the fungus *Neurospora crassa*, the nematode *Caenorhabditis elegans*, and cultured mammalian cell lines. In particular, assembly studies in rodent and human ND-subunit mutant cell lines have demonstrated

that subassemblies of nDNA-encoded subunits could be formed in the absence of mtDNA-encoded subunits (Bourges et al. 2004; Potluri et al., 2004). Cells lacking mtDNA, which lose all of the mtDNA-encoded subunits, maintain the levels of some nDNA-encoded subunits of the peripheral subcomplex that consists of, at least, NDUFS2, NDUFS3 and NDUFS8 (Bourges et al. 2004). Therefore, it has been suggested that the presence of the mtDNA-encoded subunits is not required for the formation of the peripheral arm subcomplex (Potluri et al., 2004). However, the entry points of the mtDNA-encoded subunits in the assembly process and their roles in the stability of the complex had remained elusive. Recent research using several mouse cell lines deficient for ND4, ND6, and a combination of ND6 and ND5 proposed five entry points of the mtDNA-encoded subunits in the complex I assembly process (Perales-Clemente et al., 2010). This study defined a first entry point for ND1 in the ~400 kDa-subcomplex and a second entry point for ND2, ND3 and ND4L in the ~460 kDa-subcomplex. Subsequently, ND4, ND6 and ND5 appear to be incorporated into complex in order at a third, fourth and fifth entry point, respectively. Others interesting studies on Chinese hamster cells clarified the function of some subunits in the assembly process (Scheffler et al., 2004), as that of NDUFA1 (Yadava et al., 2002). The insertion and stabilization of NDUFA1 in the mitochondrial inner membrane were shown to require mtDNA-encoded subunits, in particular, ND4 and ND6 (Yadava et al., 2004). NDUFA1 is also unstable in the absence of other membrane domain subunits like NDUFB11 (Scheffler et al., 2004). Chinese hamster fibroblasts also revealed that the stability of the peripheral arm subunits NDUFS1, 2, 3, 7, 8 and NDUFV1 and NDUFV2 were unaffected by the absence of NDUFA1, although holo-complex I was not assembled (Scheffler et al., 2004). These data suggest that the peripheral arm can be assembled in the absence of the membrane arm, similar to its assembly in *N. crassa* (Tuschen et al., 1990). NDUFA1 was also suggested to form an assembly intermediate consisting of mtDNA- and nDNA-encoded subunits and to serve as a membrane anchor to which membrane subunits are attached during complex I assembly (Yadava et al., 2004). Furthermore, recent bioinformatic analyses of the co-evolution of complex I subunits coupled with yeast two-hybrid studies revealed the interaction of human NDUFA1 with ND1 and ND4, and the interaction of human NDUF2 with ND4 (Gershoni et al., 2010). The findings reinforce the important role of NDUFA1 in

forming an assembly intermediate composed of mtDNA- and nDNA-encoded subunits. The direct physical interaction between NDUFC2 and ND4 indicates that these subunits may be incorporated into the membrane arm together. Since ND1, ND4 and NDUFA1 are essential for the assembly of the membrane arm of complex I, NDUFC2 may be also important for the assembly process. Other supernumerary subunits have also been proposed to assist in complex I biogenesis and support its structural stability, as NDUFS5, NDUFB7 and NDUFA8 (Szklarczyk et al., 2011). Besides, the assembly process of a such large number of subunit into the mature holo-complex I involves a number of assembly factors. These assembly factors are not part of the final structure of the holo-enzyme, but they are involved in biogenesis process and are found in some complex I intermediates, indicating their functions in complex I assembly/stability.

To summarize research findings about the biogenesis of complex I in mammals, Mimaki and colleagues recently (2011) proposed the assembly model illustrated in figure 10. In the early assembly stage, the core subunits NDUFS2 and NDUFS3 form a small hydrophilic assembly complex, which further expands by the incorporation of the other hydrophilic subunits, like NDUFS7, NDUFS8, and later, possibly NDUFA9. This peripheral complex is anchored to the membrane by the assembly factors Ndufaf3 and Ndufaf4 (Saada et al., 2009). The complex combines with a small membrane complex containing the mtDNA-encoded ND1 subunit, for which C20orf7 is involved in assembly or stability (Sugiana et al., 2008), to form a ~400-kDa assembly intermediate (Lazarou et al., 2007). This ~400-kDa complex incorporates with a ~460-kDa membrane complex containing ND3, ND6, ND2, ND4L and NDUFB6 to form a ~650-kDa complex under the presence of the assembly factors of Ndufaf1, Ecsit and ACAD9 (Sugiana et al., 2008). With the association of another membrane complex containing ND4, ND5 and possibly NDUFC2, an ~830 kDa assembly intermediate is formed (Gershoni et al., 2010). The assembly factor Ndufaf2 is associated with this ~830 kDa-complex and would be required in the late stage of CI assembly (Hoefs et al., 2009). Meanwhile, a hydrophilic complex, the NADH: dehydrogenase module, is built with some nDNA-encoded subunits that are directly or indirectly involved in binding and oxidizing NADH. With the addition of the NADH:dehydrogenase module and the remaining subunits, the mature holo-complex I is assembled. In this complicated and

elaborate assembly process, more assembly factors with unknown functions including Ind1, MidA, FOXRED1 and undiscovered proteins are involved.

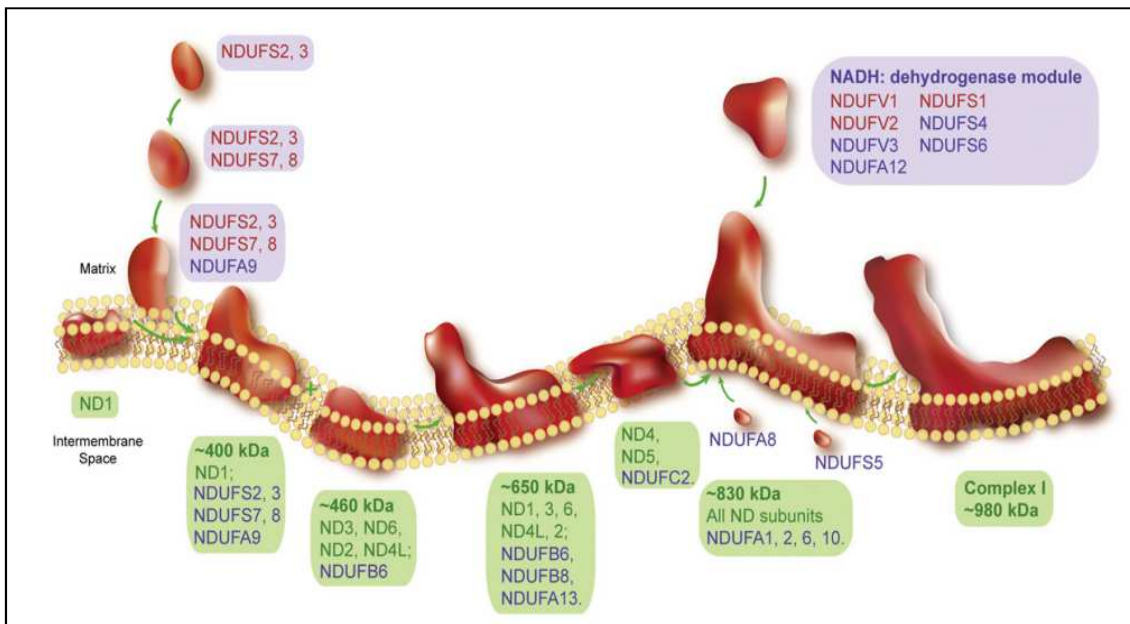


Figure 10. The assembly model of human complex I biogenesis. The initial core subunits NDUFS2 and NDUFS3 form a small hydrophilic assembly complex, which further expands by the incorporation of hydrophilic subunits such as NDUFS7, NDUFS8 and later NDUFA9. This peripheral complex, together with a small membrane complex containing mtDNA-encoded subunit ND1, forms a ~400 kDa assembly 2intermediate. This ~400 kDa complex incorporates with a ~460 kDa membrane complex containing ND3, ND6, ND2, ND4L and NDUFB6 to form a ~650 kDa complex. With the association of another membrane complex having ND4, ND5 and probably NDUFC2, an ~830 kDa assembly intermediate is formed. Meanwhile, a hydrophilic complex, NADH: dehydrogenase module (N module) is assembled by some nDNA-encoded subunits directly or indirectly involved in binding and oxidizing NADH. With the addition of the N module and remaining subunits (such as the intermembrane space subunits NDUFA8 and NDUFS5), mature complex I is assembled. The core subunits are colored with red, the rest of nDNA-encoded subunits are colored with blue. The mtDNA-encoded-subunits are in green. From Mimaki et al., 2011.

Aims

Mitochondrial diseases encompass a large assemblage of clinical disorders, commonly involving tissues with high energy requirements, such as retina, brain, heart, muscle, liver and endocrine system. Moreover, mitochondrial dysfunctions also contribute directly or indirectly to the aging process and tumor formation. Approximately 300 mtDNA alterations have been identified as the genetic cause of mitochondrial diseases, and one-third of these alterations are located in the coding genes for OXPHOS proteins. Although the understanding of the pathogenesis of mitochondrial disorders has improved considerably in the last decade, the most disappointing area is the lack of efficient treatments for the patients. Indeed, they are still treated with vitamins and cofactors mixture, which are harmless but largely inadequate and inefficient (DiMauro and Mancuso, 2007).

In the last years, a gene therapy was proposed and tried *in vitro* as a potential therapeutic option, namely allotopic expression. The term indicates the nuclear expression of the corrected wild-type mtDNA subunit engineered for mitochondrial import, which once transferred within mitochondria may compete with the native mutant mtDNA subunit to complement the biochemical defect (Gray et al., 1996). This strategy has been applied, for example, to the LHON and NARP mutations: *in vitro* studies have in fact reported the successful complementation of the OXPHOS phenotype in transmitochondrial cytoplasm hybrid (cybrid) cell lines (Manfredi et al., 2002; Guy et al., 2002), but subsequent studies compromised these results (Oca-Cossio J et al., 2003; Perales-Clemente E et al., 2011), due to the lack of convincing evidence showing that the mitochondrial defect complementation was really achieved by allotopic expression. Perales-Clemente and co-workers demonstrated in fact how an apparent functional complementation can also depend on selection of revertant mtDNA genomes. Our research group has previously characterized cybrid cell models harboring the homoplasmic disruptive m.3571insC *MTND1* mutation typical of oncogenic tumors, showing that it provokes complex I disassembly *in vitro* (Bonora et al., 2006), and *in vivo* (Porcelli et al., 2010). We also demonstrated that complex I disassembly induced an increased α -ketoglutarate/succinate ratio, due to inhibition of NADH oxidation to NAD⁺, which ultimately leads to chronic HIF1 α degradation (pseudonormoxia) and to a reduced tumorigenic potential in two different types of cancer, such as osteosarcoma and thyroid carcinoma. The m.3571insC *MTND1* mutation exhibits a threshold effect on

tumor development, because reduction of tumorigenesis is displayed only when the mutation load is above a well defined value. These findings allowed us to define *MTND1* gene as a novel type of tumor-implicated gene, named by us the double-edged oncojanus (Gasparre et al., 2011). Indeed, when m.3571insC *MTND1* mutation load is below the threshold, we demonstrate that complex I is assembled, HIF1 α is stabilized and *in vivo* tumor growth of osteosarcoma and thyroid carcinoma is increased. We show in this way the pivotal role of complex I during tumor onset in at least two tumor models.

We believe that the rescue of complex I assembly and function in our homoplasmic cybrid model, by allotopic expression of the wild type ND1 protein, can be considered indisputable. That because m.3571insC *MTND1* mutation causes the translation of a truncated ND1 subunit, then degraded, and for this reason unable to compete with the nuclear-coded one, so avoiding ambiguous results. Besides, we took advantage by a previously optimized combination of methods for the detection of low levels of m.3571insC *MTND1*, to ascertain the mutation reversion, thus allowing us to discriminate false positives allotopic clones from revertants. Achieving this goal would allow us to obtain two important results, namely to make finally feasible and reproducible the allotopic expression technique and also to further confirm our previous results on complex I implication in tumorigenesis process.

Materials and methods

Cell cultures and growth conditions

Cybrids OS-93 bearing the m.3571insC in *MTND1* gene (93% of mutation load) were generated from human osteosarcoma 143B.TK cells and previously characterized (Porcelli et al., 2010). OS-93^{ND1} cell clone was obtained after stable transfection of OS-93 with recoded ND1 construct. A previously characterized (Porcelli et al., 2010) parental control cybrid (CC), homoplasmic wild-type for the m.3571insC, was also used. OSC-93 and OSC-93^{ND1} were derived from xenografts after in vivo injection of OS-93 and OS-93^{ND1} cells, respectively. All cell lines were grown in Dulbecco's modified Eagle's medium (DMEM) with 10% FBS, 2 mmol/L L-glutamine, 100 units/mL penicillin, 100 µg/mL streptomycin, 0.1 mg/mL bromodeoxyuridine, and 50 µg/mL uridine. Cultures were grown in a humidified incubator at 37° C with 5% CO₂. All cell lines were authenticated by mtDNA genotyping. Occurrence of the m.3571insC mutation and accurate quantification of heteroplasmy levels as previously described (Kurelac et al., 2010) were verified before and after explant as well as before each in vitro experiment.

ND1 construct and clone stable generation

Human mitochondrial *MTND1* gene was nucleus-recoded and engineered in p3XFLAG-CMV-14 vector in the Laboratorio di Genetica Medica (Sant'Orsola Hospital, Bologna). Recoded ND1 construct was transfected in OS-93 cell line and transfection was carried out with Lipofectamine2000 (Invitrogen, Milan, Italy) following manufacturer's instructions.

After 24h, cells were incubated in a medium containing the 500ug/ml G418 antibiotic and ten cell clones were isolated. These clones were incubated in glucose-free DMEM supplemented with 5 mmol/L galactose, 5 mmol/L Na-pyruvate, and 10% FBS (DMEM-galactose) for 24h, in order to select only those cells able to use oxidative phosphorylation through the restore of complex I assembly and function. Under this condition, two cell clones were isolated, namely OS-93^{ND1-B} and OS-93^{ND1-C}.

Cell viability measurements

Cells (3×10^4) were seeded into 24-well plates and, after 24 hours, incubated in DMEM-galactose. Cell viability was determined by the colorimetric sulforodhamine B (SRB) assay, following the manufacturer's conditions. Briefly, at the end of incubation time, cells were fixed with 50% trichloroacetic acid (TCA) for 1 hour at 4°C, washed 5 times with H₂O and finally dried for 1 hour at room temperature. Cells were then stained with SRB 0.4% diluted in 1% acetic acid for 30 min at room temperature, washed 4 times with 1% acetic acid, and disrupted with 10 mM Tris-HCl pH 9.8. The absorbance of SRB was detected with Victor3 plate reader (Perkin Elmer) at the wavelength of 560 nm.

SDS-PAGE and Western blotting

Digitonin-isolated mitochondria were prepared from 5×10^6 cells and resuspended in PBS containing 2% DDM. After 15 min of incubation in ice, the sample was centrifuged for 30 min at 13 000 g (4°C) and the supernatant was mixed with an equal volume of tricine sample buffer containing 2% (v/v) 2-mercaptoethanol. The mixture was kept at room temperature for 60 min. Protein (50 µg protein/lane) was separated on 10% polyacrylamide gel and transferred on nitrocellulose membrane (Bio-Rad) that were subsequently incubated with primary antibody against ND1 (1:1000, a gift from A. Lombes, Unite de Recherche INSERM 153, Hospital de la Salpetriere, Paris, France), NDUFV1 (1:1000, Sigma-Aldrich) and VDAC (1:1000, BioVision, Mountain View, CA, USA). Peroxidase-conjugated anti-rabbit IgGs secondary antibodies were used (1:2000, Jackson Immunoreaserch). Chemiluminescence signals were measured with a Kodak molecular imaging apparatus (Kodak, Rochester, NY, USA).

2D Blue Native-SDS PAGE and western blotting

Strips from the first dimension Blue Native electrophoresis were used for 2D-SDS electrophoresis as reported in (Calvaruso et al. Methods 2008). Western blotting analysis was performed as above.

Clear Native Electrophoresis (CNE) and in gel activity assay

Digitonin-isolated mitochondria were solubilized using 0.4% (w/v) n-dodecyl- β -D-maltoside (DDM) and 100ug of proteins were separated on 5-13% gradient polyacrylamide gel (Wittig et al., 2006). Complex I IGA was determined by incubating the gel with 2 mM Tris-Cl (pH 7.4), 0.15 mM NADH, and 2.5 mg/ml MTT at room temperature for 1 h. The reaction was stopped with 50% methanol and 10% acetic acid, and the gel was analyzed with a Kodak molecular imaging apparatus (Kodak, Rochester, NY, USA).

ATP synthesis measurement

The measurements of mitochondrial ATP synthesis were done in cells grown in DMEM-glucose according to Manfredi et al. 2002b, with minor modifications. Briefly, after trypsinization, cells were resuspended (7×10^6 /mL) in buffer A [10 mM KCl, 25 mM Tris-HCl, 2 mM EDTA, 0.1% bovine serum albumin, 10 mM potassium phosphate, 0.1 mM MgCl₂ (pH 7.4)], kept for 15 minutes at room temperature, and then incubated with 50 μ g/mL digitonin for 1 min. After centrifugation, the cells pellet was resuspended in buffer A and aliquots were taken to measure ATP synthesis, protein content, and citrate synthase activity. Aliquots of cells were incubated with 5 mM malate plus 5 mM pyruvate (complex I-driven substrates) in the presence or absence of 10 μ g/mL oligomycin, or with 10 mM succinate plus 2 μ g/mL rotenone (complex II-driven substrate). The reaction was started by addition of 0.2 mM ADP in the presence of luciferine/luciferase, as detailed by the Sigma Aldrich kit manufacturer's instructions, and chemiluminescence was determined as a function of time with a luminometer. After addition of 10 mM oligomycin, the chemiluminescence signal was

calibrated with an internal ATP standard. The rate of ATP synthesis was expressed as a ratio of citrate synthase activity (Trounce et al., 1996). Protein concentration was determined according to Bradford (Bradford, 1996).

In vivo studies

Cells (3×10^6) were suspended in 0.2ml sterile PBS and injected subcutaneously in immunodeficient 4-7 week-old athymic Crl:CD-1-*Foxn1*^{nu/nu} mouse strain (referred to as *nude* mice, purchased from Charles River, Italy). Experiments were authorized by the Institutional Review Board of the University of Bologna and performed according to Italian and European guidelines. Individually tagged virgin female mice (5-15 per experimental group) were used. Tumor growth was assessed with a caliper; volume was calculated as $\pi[\sqrt{(a*b)}]^3/6$, where a=maximal tumor diameter, and b=tumor diameter perpendicular to a. Lungs were stained with black India ink and fixed in Fekete's solution to better outline metastases, which were then counted using a dissecting microscope.

Immunohistochemistry

Immunohistochemical staining (IHC) was performed on paraffinized xenograft sections, which were dewaxed, rehydrated, and retrieved using a Tris-EDTA pH 9.0 solution (20 min at 98°C). Endogenous peroxidase activity was quenched with a methanol/H₂O₂ 1,5% solution.

Primary antibodies against MTND6 complex I subunit (Invitrogen, Milan, Italy) and HIF1 α (Upstate Biotech, Billerica, MA, USA) were incubated overnight and processed with a non-biotin-amplified system (NovoLink, Milan, Italy) according to the manufacturer's instructions. The reaction was developed with 3-3'-diaminobenzidine tetrahydrochloride/H₂O₂ solution. Sections were counterstained with hematoxylin, dehydrated and mounted in Bio-Mount (Bio-Optica, Milan, Italy).

TCA metabolites extraction and measurement

Metabolites α -KG and SA were extracted from tumors (35mg) in cold methanol /chloroform/water in a ratio of 2:1:0.7 in presence of $^{13}\text{C}_4$ succinic acid as internal standard. Sample was maintained on ice for 5min, vortexed twice and centrifuged for 5min at 3000rpm at 4°C. To the upper phase, chloroform/water in a ratio 1:1 was added and sample was vortexed and centrifuged for 5min at 3000rpm at 4°C. The upper phase was separated from the lower organic phase and lyophilized. Samples were then analyzed by mass spectrometry.

Electron microscopy (EM)

Xenograft biopsies were immediately collected and processed, as previously reported (Ambrosini-Spaltro et al., 2006). Sections (1 μm) were stained with 1% toluidine blue for morphology control and EM area selection. Thin sections were observed with JEM-1011 Transmission Electron Microscope (Jeol, Ltd). For each xenograft at least two different areas were analyzed to rule out intratumor heterogeneity.

Pimonidazole staining

Animals were injected intraperitoneally with 60mg/kg pimonidazole (Hypoxyprobe-1 Plus Kit, HPI, Burlington, MA) 3h prior to sacrifice. Xenografts were snap-frozen and cut in 10 μm slices. Tissues were fixed for 20min with cold acetone, kept for 1h with PBS containing 5% FBS and incubated for 1h with FITC-MAb1 antibody (1:10). Fluorescence was visualized with a digital imaging system using an inverted epifluorescence microscope with 63X/1.4 oil objective (Nikon Eclipse Ti-U, Nikon, Japan) at 488nm. Images were captured with a back-illuminated Photometrics Cascade CCD camera system (Roper Scientific, Tucson, AZ, USA) and elaborated with Metamorph acquisition/analysis software (Universal Imaging Corp., Downingtown, PA, USA).

Fluorescent PCR

Fluorescent PCR reaction was performed using AmpliTaq Gold polymerase (Applied Biosystems, Foster City, CA, USA) with a fluorescently labelled forward primer (Kurelac et al, 2011). PCR products were loaded onto 3730 DNA Analyzer together with GeneScan 500 Liz Size Standard following the manufacturer's instructions. Analysis was performed by GeneMapper v.3.5 and peak parameters were evaluated by Peak Scanner (Applied Biosystems, Foster City, CA, USA).

Denaturing High Performance Liquid Chromatography

WAVE 208 Nucleic Acid Fragment Analysis System (Transgenomic, Omaha, NE) was applied for the mutant load evaluation with DHPLC. PCR reaction was performed with AmpliTaq gold polymerase (Applied Biosystems, Foster City, CA, USA) using a forward and reverse primers and the amplification product was separated using 61,1° C separation temperature (Kurelac et al, 2011).

RNA extraction and Real Time analysis

RNA was extracted from snap-frozen tissues with RNeasy Plus Mini kit (Qiagen, Milan, Italy) and cDNA was prepared using SuperScript III Reverse Transcriptase (Invitrogen, Milan, Italy) following manufacturers' instructions. Expression of *GLUT-1*, *VEGF-A* and *LDHA* was analyzed with Real Time PCR using Sybr Green chemistry and 7500 Fast Real Time System (Applied Biosystems) as previously described (Gasparre et al, 2011).

Statistics

SigmaStat 3.5 software was used for statistical analysis applying Student's t-test unless otherwise indicated.

Results

Allotopic *MTND1* expression strategy

Human mitochondrial *MTND1* gene was nucleus-recoded and engineered in p3XFLAG-CMV-14 vector in the Laboratorio di Genetica Medica (Sant'Orsola Hospital, Bologna). To optimize the efficiency of allotopic expression, the ND1 mRNA was targeted to the mitochondrial surface, thus ensuring tight coupling between both translation and translocation processes of the highly hydrophobic corresponding polypeptide. To achieve that, the engineered *ND1* gene was combined with the *cis*-acting elements of the *COX10* gene, which ensures the efficient sorting of the mRNAs to the mitochondrial surface (Sylvestre J. et al., 2003; Bonnet C. et al., 2007; Bonnet C. et al., 2008). Hence, the MTS (mitochondrial targeting sequence) and COX10 3' UTR (untranslated region) were added in frame at the N- and C-terminal of the protein, respectively (Fig.11). Moreover, a FLAG epitope was appended at the C-terminal.

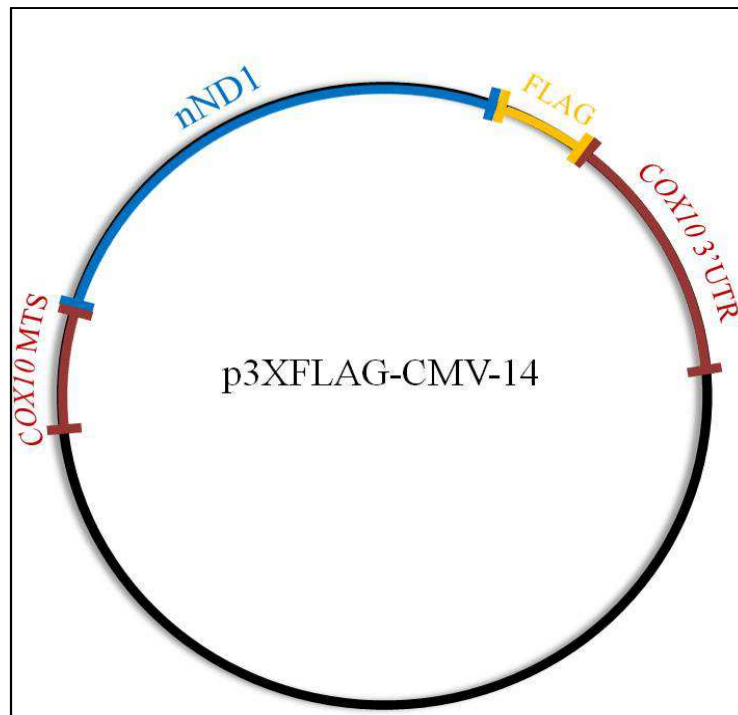


Figure 11. Schematic *ND1* construct.

Allotopic ND1 expression restores the energetic efficiency in cells bearing m.3571insC *ND1* mutation

The ND1 construct was transfected in OS-93 osteosarcoma cybrid line, bearing homoplasmic m.3571insC *MTND1* mutation. This frame-shift mutation causes the translation of a truncated ND1 protein, which is subsequently degraded and induces complex I disassembly. Therefore, due to the lack of respiratory chain complex I, OS-93 cell line is characterized by a severe energetic impairment (Porcelli AM et al., 2010).

After transfection, ten stable cell lines were isolated by antibiotic selection and then incubated in a glucose-free medium containing galactose, in order to select those cells with an efficient oxidative phosphorylation, resulting from successful restoration of complex I function/assembly. Two cell clones, OS-93^{ND1-B} and OS-93^{ND1-C}, were significantly more viable in galactose medium than OS-93, suggesting their capacity to rely solely on oxidative phosphorylation for energy production (Fig. 12). Conversely, we previously demonstrated that OS-93 cells are unable to grow in galactose medium, (Porcelli AM et al. 2010).

The precise *MTND1* mutation load was measured by fluorescent PCR (Kurelac I. et al., 2011), in collaboration with the Laboratorio di Genetica Medica. The *MTND1* mutation was virtually homoplasmic in OS-93 and OS-93^{ND1-B}, whereas the OS-93^{ND1-C} clone was a revertant (Fig.13), and therefore it was excluded by further analysis. Moreover, by sequencing the whole gene, clone was repeatedly confirmed not to accumulate additional *MTND1* mutations that may complement the m.3571insC for example *via* the recovery of the reading frame.

In order to verify that ND1 protein was translated and imported into mitochondria, Western blot analysis was performed on control (CC), OS-93 and OS-93^{ND1} cybrid clones. The ND1 protein was detected in the mitochondrial fraction from CC and OS-93^{ND1} only (Fig.14A), clearly indicating successful allotopic expression. Moreover, to assess whether the complex I assembly was restored in OS-93^{ND1} cybrid clone, mitochondria were separated by 2D BN/SDS PAGE, further processed by western blot and incubated with antibody against ND1 (Fig. 14B) and the nuclear subunit NDUFV1 (Fig. 14C). Both subunits were detected in OS-93^{ND1} in the fully assembled complex I. The complex I function was then determined by the in-gel activity (IGA) assay. As shown in Fig. 14D, the complex I IGA was fully restored upon ND1 allotopic

expression. Finally, the rate of rotenone-sensitive ATP synthesis was markedly increased in OS-93^{ND1}, clearly indicating that complex I function was recovered (Fig.15). Conversely, no difference in complex II-driven synthesis was observed, suggesting that the effect of allotopic expression was specific for complex I (Fig.15).

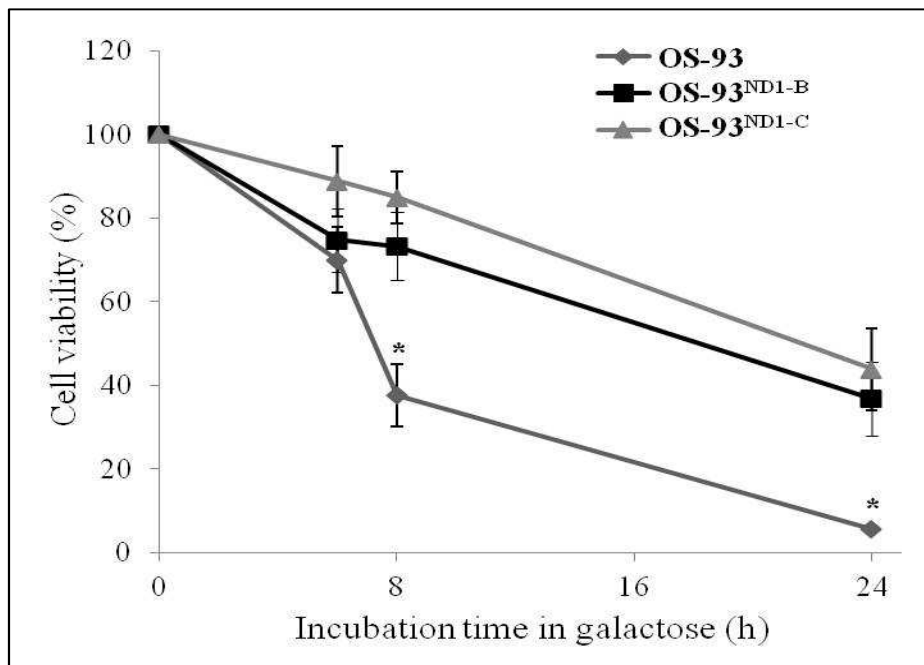


Figura 12. Viability in galactose medium. The cell lines were incubated in DMEM containing galactose for indicated times and viability was determined by SRB assay. Data represents the media \pm SEM (n=4) and statistics was defined by STUDENT t-test ($p < 0,05$).

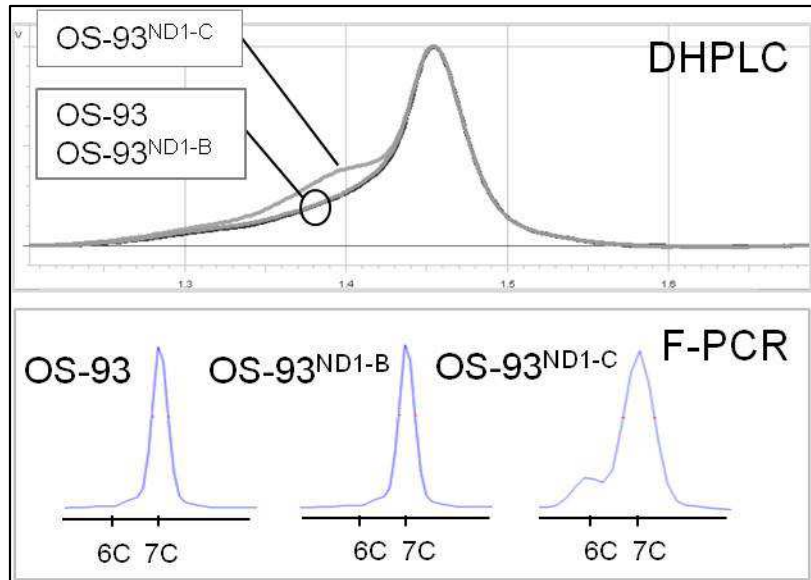


Figure 13. ND1 mutation heteroplasmy level measured by DHPLC and fluorescent PCR.

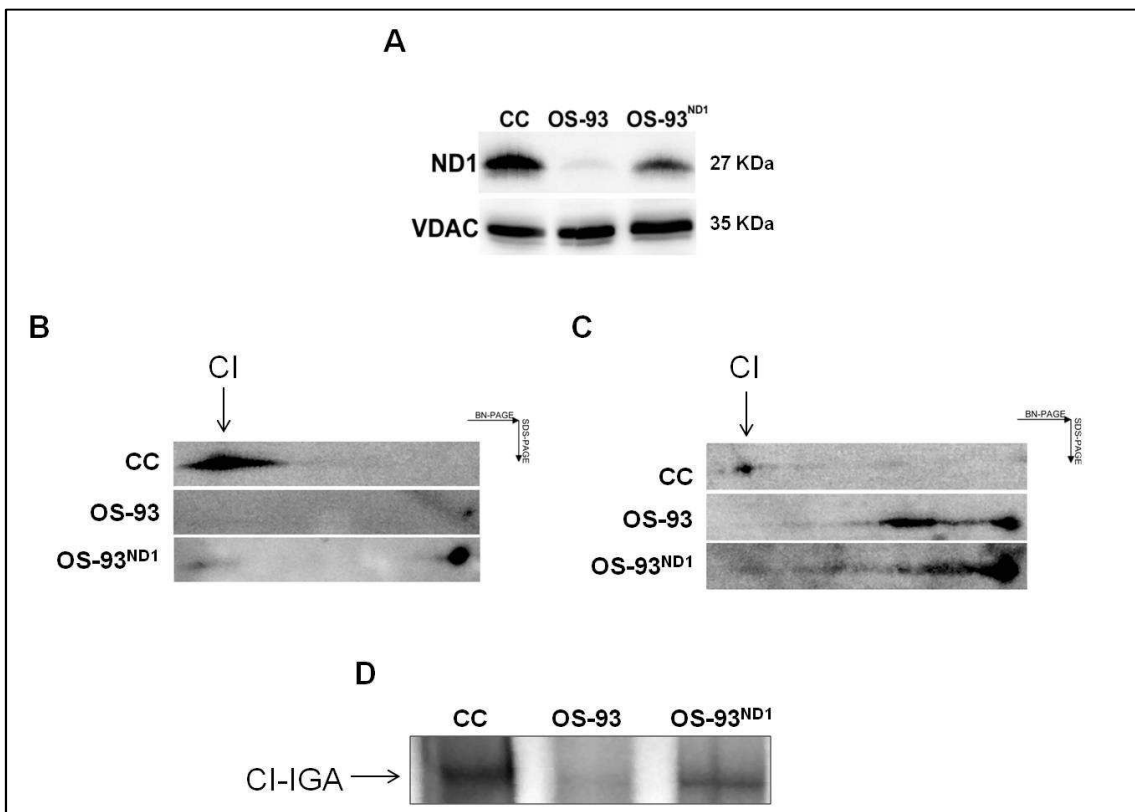


Figure 14. Complex I subunits content and in-gel activity (IGA) of isolated mitochondria fractions. A) Western blot for ND1 protein in CC (cybrid control), OS-93 and OS-93^{ND1}. VDAC was used as a mitochondrial loading control. Western blot analysis of complex I assembly using ND1 (B) and NDUFV1 (C) antibodies, respectively. D) Complex I IGA assay on CC, OS-93 and OS-93^{ND1}.

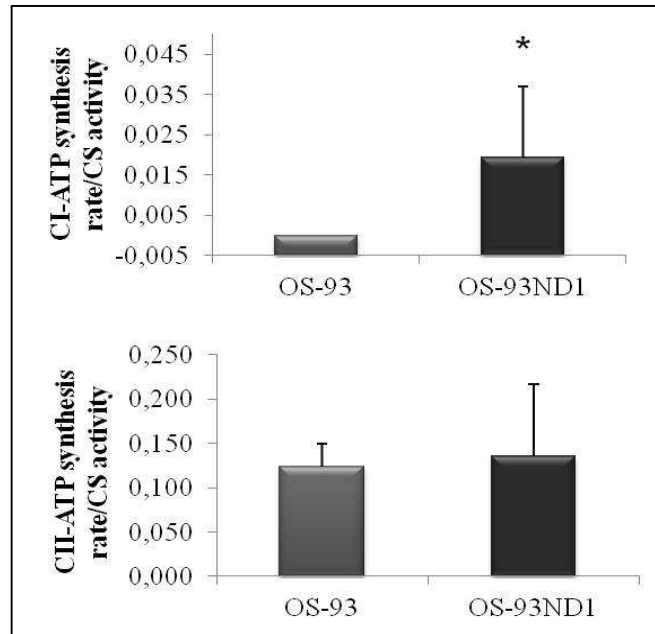


Figure 15. Mitochondrial ATP synthesis by complex I (upper) and by complex II (bottom) was determined in digitonin-permeabilized cells in presence of pyruvate/malate and succinate, respectively. Rates, normalized by citrate synthase (CS) activity of corresponding sample, are mean ($n=4$) \pm SD.

ND1 allotopic expression rescues tumorigenic potential of OS-93 cell line

We previously demonstrated that m.3571insC *MTND1* in OS-93 cells hampers tumor growth *in vivo* due to the complex I disassembly and consequent HIF1 α destabilization (Gasparre et al., 2011).

To assess if the *in vivo* tumorigenic potential of OS-93 cells was rescued by ND1 allotopic expression and complex I assembly/function recovery, we injected OS-93 and OS-93^{ND1} in *nude* mice. OS-93^{ND1}-derived tumors grew significantly larger than OS-93-derived ones (Fig. 16A).

No other mutation was detected in xenografts upon re-sequencing the whole mtDNA apart from m.3571insC *MTND1*. Complex I IGA was detected only in xenografts derived from OS-93^{ND1} cells but not in OS-93 derived tumor. These results clearly demonstrate that complex I assembly and function are required to increase tumorigenic potential *in vivo*.

Complex I recovery by ND1 allotopic expression hampers oncogenic transformation

The m.3571insC *MTND1* is a hallmark of oncogenic lesions together with similar truncating mutations mainly occurring in homoplasmy (Bonora et al., 2007; Porcelli et al., 2010). We demonstrated that this mutation is sufficient to induce oncogenic transformation when above threshold (disassembled complex I), but not when below threshold (complex I is properly assembled and able to cope with tumor energetic requirements) (Gasparre et al., 2011).

Then we verified whether an inactive and disassembled complex I was required for oncogenic transformation. Indeed, electron microscopy analysis showed increased mitochondria number and swollen morphology (Fig.17) on xenograft of OS-93, that is typical of an oncogenic look. These data therefore confirmed that the presence of a functioning complex I hampers oncogenic transformation.

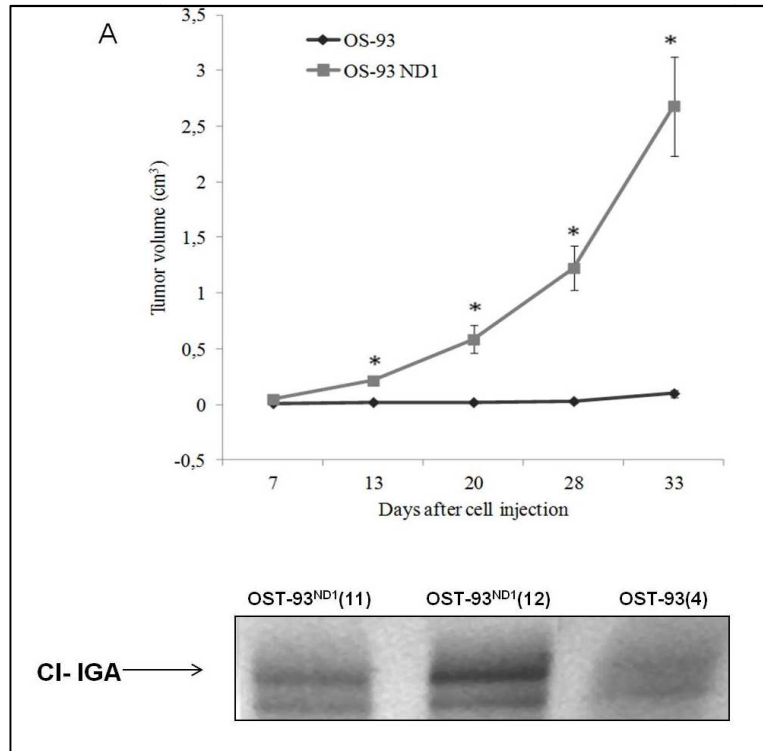


Figura 16. A. Tumor growth generated by injection of OS-93 and OS-93^{ND1} in nude mice. Data are means of two experiments each with 5 animals \pm SEM; *, $P < 0,01$. B. Complex I IGA on OS-93 and OS-93^{ND1} derived xenografts after explant (OST, OS tumor). One representative experiment of four is showed.

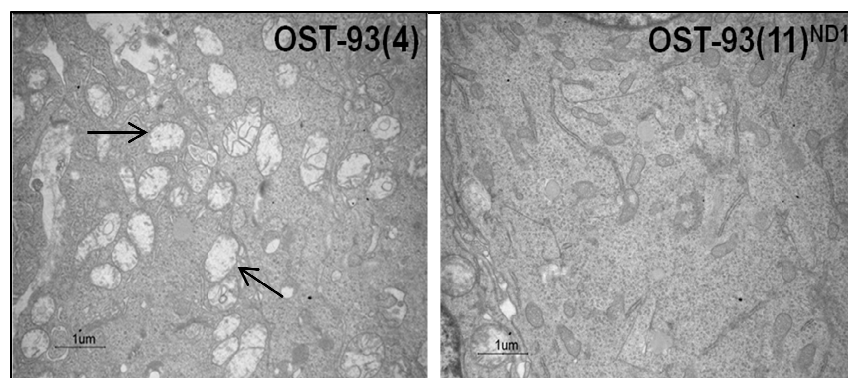


Figura 17. Electron microscopy on xenografts after explants. (4) and (11) indicate mouse-xenograft number. Oncocytic phenotype is apparent in OS-93(4) tumor by increased mitochondria number, swollen mitochondria morphology and disorganized cristae (arrows indicate some examples). That set up is not present in allotopic tumors, whose OST-93^{ND1}(11) is a representative case.

Hif1 α -stabilization is involved in increased tumor growth

In order to assess whether the increase of tumorigenic potential of OS-93^{ND1} *in vivo* requires HIF1 α stabilization tumor growth, immunohistochemistry analysis was performed on xenografts. Staining of MTND6 complex I subunit and HIF1 α was positive only in OS-93^{ND1}-derived tumors, whereas it was negative in OS-93-derived one (Fig. 18A) indicating a strong association between HIF1 α and MTND6 expression (Fig.18B). As we previously showed, HIF1 α destabilization due to the complex I disassembly, is associated to an imbalance of the TCA α -ketoglutarate (α KG) and succinate intermediates (Porcelli et al., 2010; Gasparre et al., 2011). This imbalance favours accumulation of the first one, thus increasing the ratio α KG/succinate, promoting HIF1 α -hydroxylation by PHD and consequently causing its proteasomic degradation. To verify whether this imbalance was reverted by ND1 *in vivo* allotypic expression, the α KG/SA ratio was determined after metabolites extraction from xenografts and measurement by mass spectrometry. α KG/SA ratio was significantly higher in OS-93 xenograft compared to OS-93^{ND1} ones (Fig. 18C), demonstrating that the balance of these TCA cycle metabolites depends on proper activity of complex I. Besides, to evaluate whether HIF1 α stabilization in OS-93^{ND1} tumors could have induced some functional consequences on downstream gene expression, the expression of its responsive genes was determined. An increased expression of glucose transporter-1 (*GLUT1*), vascular endothelial growth factor A (*VEGFA*) and lactate dehydrogenase A (*LDHA*) was detected in these tumors only (Fig.19A). Moreover, staining with hypoxic marker pimonidazole (Chen Y. et al., 2009) showed some greater hypoxic areas in OS93-derived small tumor in comparison to that OS93^{ND1} derived larger ones (Fig.19B), highlighting that HIF1 α stabilization was prevented in complex I deficient tumors, despite to a real hypoxic condition.

Biochemical effect of ND1 allotopic expression is also preserved in *ex vivo* cell lines

To point out and further verify ND1 allotopic expression effect, additional analysis has been made also in *ex vivo* cell lines. Cell lines were isolated from single very small OS-93 derived xenograft, namely OSC-93(4), and from the four largest OS-93^{ND1} xenografts, namely OSC-93^{ND1}(11), (12), (17) and (19). It was verified by F-PCR that they were not revertants and then they were biochemically analyzed. During incubation in galactose medium, the cell viability was significantly lower for OSC-93(4) compared to OSC-93^{ND1}(11), (12), (17) and (19) (Fig. 20A), whereas western blot experiments showed ND1 protein presence only in mitochondrial fraction of OSC-93^{ND1}(11), (12), (17), (19) (Fig. 20B). Unfortunately, cyclic heteroplasmy level measuring by F-PCR showed that OSC-93^{ND1}(17) and (19) was turned into revertants, probably due to a mutation shift versus wild type occurred during cell growth in medium culture. For this reason, they were not considered for further analysis. Instead, OSC-93(4), OSC-93^{ND1}(11) and OSC-93^{ND1}(12) cell lines were analyzed by 2D BN/SDS PAGE and by IGA experiments to verify that ND1 allotopic protein was correctly inserted in complex I. Figure 21 shows that complex I was assembled and active in OSC-93^{ND1}(11) and OSC-93^{ND1}(12) but not in OSC-93(4), demonstrating that allotopic expression was maintained also in *ex-vivo* cell lines.

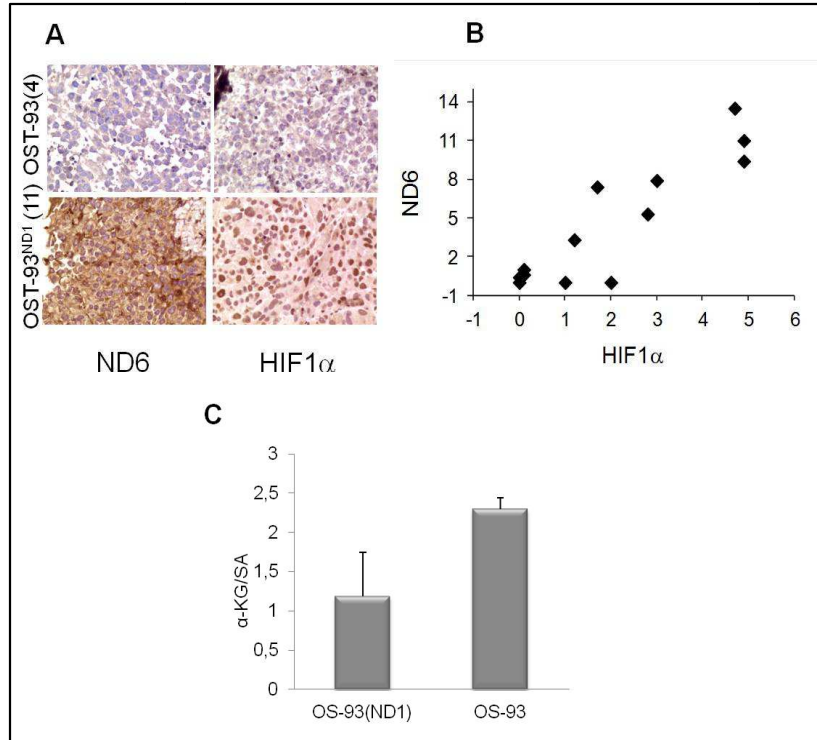


Figure 18. Recovery of complex I assembly implicates Hif1 α stabilization in OS-93^{ND1} xenografts. A. Representative IHC staining using antibodies against MTND6 and Hif1 α on OS-93 and OS-93^{ND1} dissected tumor masses and (B) linear regression from overall data. C. The ratio of α KG and SA was calculated by measuring the level of each metabolite from 3 different experiments of mass spectrometry.

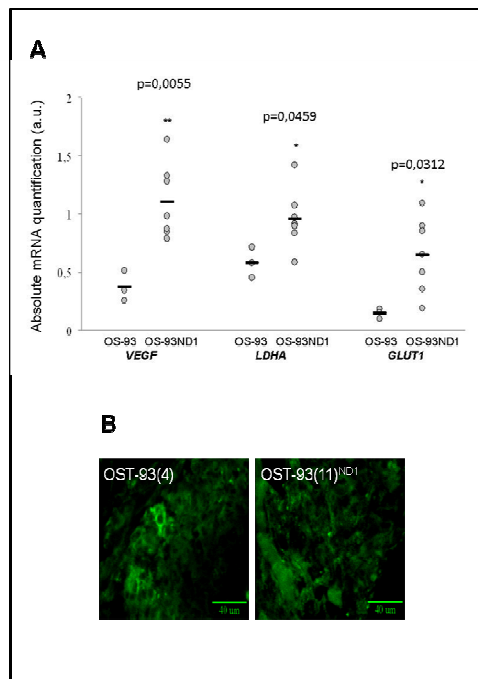


Figure 19. A. Gene expression levels of Hif1 α -responding genes observed in OS-93 and representative OS-93^{ND1} xenografts. Absolute mRNA quantification of GLUT-1, VEGF-A, and LDHA in tumors explanted from nude mice is reported (*, $P<0,05$; **, $P<0,01$). Black bars indicate the average value. B. Pimonidazole staining of OS-93 and representative OS-93^{ND1} tumors. Magnification x63.

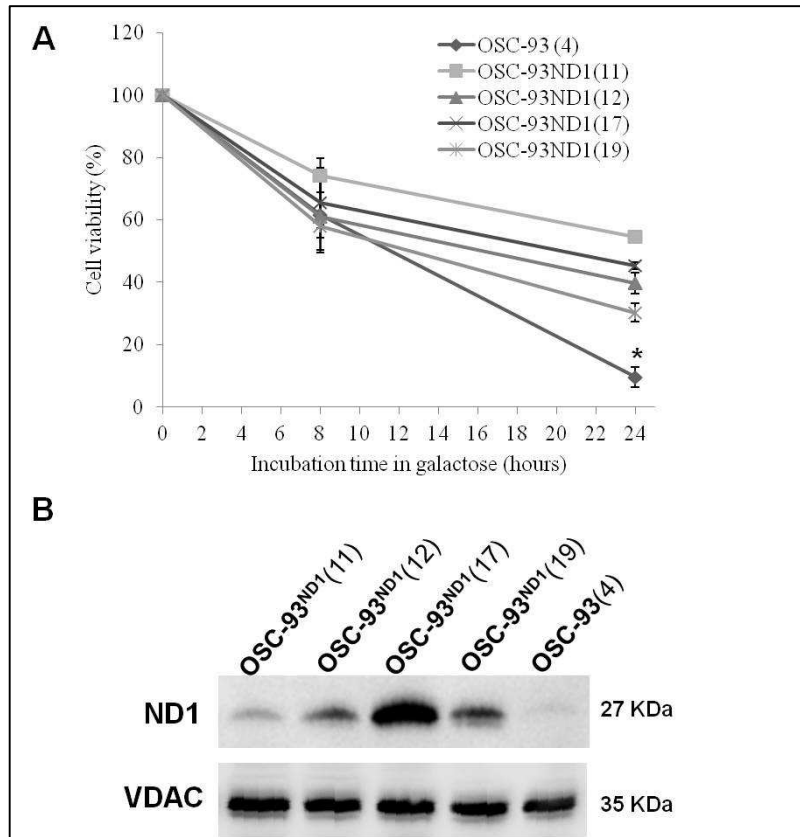


Figure 20. A. Viability in galactose medium of *ex vivo* OS-93 and OS-93^{ND1} cell lines. The cell lines isolated from xenograft after explants, were incubated in DMEM containing galactose for indicated times and viability was determined by SRB assay. Data represents media \pm SEM (n=4) and statistics was defined by ANOVA (p<0,001). B. Western Blot analysis for ND1 on mitochondrial fraction of *ex vivo* OSC-93 and OSC-93^{ND1} cell lines. VDAC was used as mitochondrial loading control.

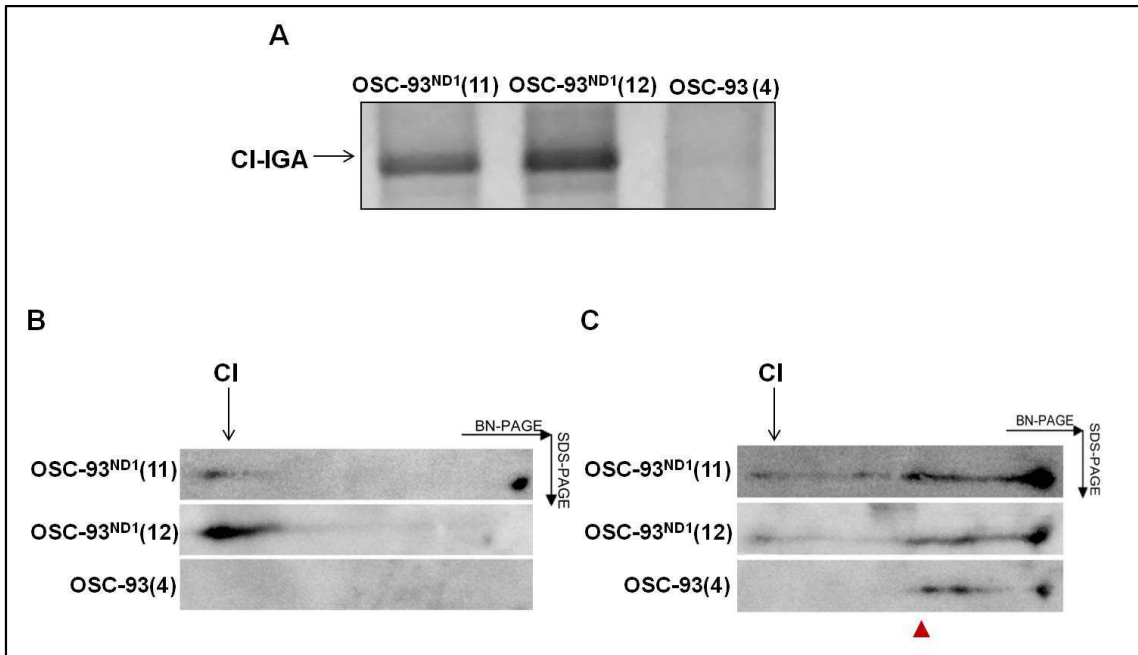


Figure 21. A. Complex I IGA assay on ex-vivo cells OSC-93(4), and OSC-93^{ND1}(11) and (12) isolated mitochondria. B. C. Western blot analysis of complex I assembly using ND1 and NDUFV1 antibodies, respectively. Antibody against NDUFV1 nuclear subunit showed the correct CI assembly in OSC-93^{ND1}(11) and in OSC-93^{ND1}(12), whereas part of the peripheral arm is accumulated in small molecular weight sub-assembled in OSC-93(4) (indicated with red triangle).

Conclusions

In the present study we achieved two important goals, in relation to the applied strategy and to the experimental results. Allotopic expression strategy was improved and further optimized in last decade with the aim to perfect a possible gene therapy for mitochondrial diseases by biochemical defect complementation. Despite this strategy has been successfully demonstrated in yeast, in mammalian mitochondria results are very controversial. In fact, available evidence is based only on partial phenotype rescue, and not on the demonstrated incorporation of a functional protein into respiratory complexes. Indeed, this apparent functional complementation has been shown also depend on selection of revertant mtDNA genomes (Perales-Clemente et al., 2010). Among all, the main critical issue for the allotopic strategy is certainly the difficult and inefficient mitochondrial import of such highly hydrophobic proteins (Oca-Cossio J. et al., 2003).

In this study, we undertook a different approach to solve the issue of feasibility of the allotopic strategy for gene therapy of mtDNA mutations and to assess its efficiency in truly complementing the biochemical dysfunction. We took advantage of the previously characterized cybrid cell models harboring the homoplasmic disruptive m.3571insC *MTND1* mutation shown to induce complex I disassembly *in vitro* and *in vivo* (Gasparre et al., 2011). In order to complement the homoplasmic m.3571insC, causing translation of truncated protein thereafter degraded, we recoded *MTND1* for cytosolic translation (nND1) by adapting codon usage via *in vitro* site-directed mutagenesis. The eukaryotic expression construct was generated with the aim to facilitate nND1 mRNA targeting to the external mitochondrial membrane according to Bonnet and co-workers (Bonnet et al., 2007). The 5'UTR containing a MTS of nuclear coded COX10 mitochondrial subunit of complex IV was cloned upstream of and in frame with nND1, while 3'UTR of COX10 was cloned downstream. Previously used vectors with a built-in MTS, in fact, are not suitable as they are designed for matrix soluble, not for membrane embedded proteins. After transfection of the construct in our cybrid model OS-93, knocked for ND1, and after following selection of virtually positive clones by antibiotic and by galactose medium, we addressed the issue of genetic revertants. Sensitivity of Sanger sequencing was not sufficient to exclude low levels of wild-type mtDNA copies, as the threshold for phenotypic effect of disruptive mutations has been shown by us to be quite high (Gasparre et al., 2011). Therefore, for the first time we here implemented

a previously optimized combination of methods for the detection of low levels of m.3571insC (Kurelac I. et al., 2011), an analysis that has lacked so far, in the attempt to ascertain the mutation reversion (Perales-Clemente et al., 2010). We obtained the precise load of mutant mtDNA by fluorescent PCR and confirmed it by denaturing high performance liquid chromatography in the selected clones, discriminating a revertant one (not further considered) and a positive allotopic one. First, we detected correct synthesis and import to mitochondria of nND1 protein exclusively in allotopic positive clone OS-93^{ND1}, by Western blot analysis on mitochondrial fraction, using a specific ND1 antibody. Moreover, in order to verify that the nND1 subunit was assembled within complex I, we performed a two-dimensional Blue Native SDS-PAGE followed by western blotting and specific immunodetection of complex I subunits. nND1 immunoreactivity was associated with the fully assembled complex I in the positive control (CC), whereas no immunoreactivity was observed in OS-93; finally, the anti-ND1 in the OS-93^{ND1} showed the presence of the subunit in the fully assembled complex. Further confirmation of the recovery of complex I assembly came from the incubation with the anti-NDUFV1 nuclear subunit antibody, which immunoreactivity was associated with the fully assembled complex I in the positive control whereas in the OS-93 the NDUFV1 subunit was present in the monomeric form and in the small subcomplex, but not in the fully assembled complex I. Finally, NDUFV1 in OS-93^{ND1} was present in the monomeric form, in the subcomplex and also in the fully assembled complex. Moreover, complex I IGA band, detected exclusively in CC and in OS-93^{ND1}, but not in OS-93, proved that nND1 restored not only complex I assembly, but also its enzymatic activity and this was further confirmed by measurement of rotenone-sensitive ATP synthesis.

These results provide solid evidence that allotopic expression of ND1 led to its import within mitochondria and, more importantly, allowed for re-expression of assembled complex I, which could not occur with the native mutant ND1 subunit, being truncated, degraded and for this reason not expressed. Furthermore, by sequencing the whole gene, cell lines were repeatedly confirmed not to accumulate additional *MTND1* mutations that may complement the m.3571insC e.g. via the recovery of the reading frame. Moreover, the necessary exclusion that the re-assembled complex I might have occurred because of low, under the detection-level amounts of revertant wild-type mtDNA was

reasonably achieved by the implemented sensitive approach for heteroplasmy detection (Kurelac I et al., 2011).

These results offer promising expectations because, finally demonstrating without ambiguity that allotopic strategy is feasible and effective in correcting the OXPHOS defects due to mtDNA mutations, they represent a first step for a future clinical trial in patients. Furthermore, despite the limited efficiency of mitochondrial import of the allotopically expressed protein, low levels of heteroplasmy are known to be sufficient to complement the OXPHOS deficiency due to mutant mtDNA (Park and Larsson, 2011); thus, easily accessible tissues, as it is the case, for example, for retinal ganglion cells in Leber's Hereditary Optic Neuropathy (LHON), are potentially suitable to the allotopic strategy using safe and efficient vectors.

The second important goal of the present study arises from the results of OS-93 and OS-93^{ND1} cell lines injection in nude mice. We have previously demonstrated that m.3571insC, following a threshold effect, hampers *in vivo* tumor growth of cancer cells. Indeed, we identified a precise threshold for such mutation, sufficient to increase the α -KG/SA ratio, thus inducing HIF1 α destabilization, and ultimately triggering growth arrest. We previously provided the proof of principle regarding the antitumorigenic effect of a mtDNA truncating mutation by using our unique cell model (Porcelli et al., 2010) and then experimentally reinforced that through reinjection of highly isogenic clones OSC-78 and OSC-83, carrying a mutation load below and above threshold, respectively. In agreement with our previous observations in patients with oncocytic tumors (Porcelli et al., 2010), tumor xenografts bearing a mutation above threshold displayed pseudo-normoxia, showing HIF1 α destabilization despite being truly hypoxic. We have shown that this mechanism, tightly linked to the α -KG/SA imbalance as it occurs in SDH and FH mutated tumors but in opposite direction, may be sufficient to drive the tumor into a "blind alley" due to both respiratory impairment and lack of HIF1 α -dependent glycolysis induction (Gasparre et al., 2011b). Accumulation of NADH and inhibition of α -ketoglutarate dehydrogenase are likely the most plausible mechanisms for the α -KG/SA ratio increase as a consequence of complex I disassembly. This imbalance in the TCA cycle intermediates may hence either boost the PHD affinity for molecular oxygen or diminish the availability of the main allosteric inhibitor of PHD, that is SA, thus determining HIF1 α destabilization even during hypoxia.

The most important consideration come from the strong association between homoplasmic disassembling mtDNA mutations, such as the m.3571insC by us investigated in the present study, and the mostly benign oncocytic tumor phenotype. Patients with oncocytic tumors (epithelial derived tumors) rarely present highly aggressive, metastatic cancers; in the majority of cases, these tumors are surgically removed because of hindrance at the site of occurrence. Our findings provide an explanation for this clinical observation through HIF1 α destabilization, strictly correlated to complex I disassembly and, in turn, lack of activation of downstream pathways activation implicated in glycolytic metabolic shift (Warburg effect) and angiogenesis. Our studies in mice have shown that, upon trespassing the threshold, the mutation is sufficient to trigger oncocytic transformation even in a nonepithelial cancer, highlighting the importance of homoplasmy of disruptive mtDNA mutation as prognostic markers.

Obtaining an allotopic positive clone, in which complex I assembly and function were restored by complementation of m.3571insC with wild-type nND1 expression, has given us the unique opportunity to further confirm these important previous results. We expected to observe the rescue of tumorigenic potential of OS-93 cell line after expression of nND1 protein, as a consequence of complex I re-assembly and function. Accordingly, injection of two cell lines OS-93 and OS-93^{ND1} in nude mice displayed the rescue of tumor growth for the allotopic one only, in which complex I was fully assembled and active, as confirmed also by the CI-IGA assay on xenografts. Moreover, electron microscopy did not show oncocytic phenotype in OS-93^{ND1}-derived xenografts, confirming that functioning complex I hampers oncocytic transformation. As expected, HIF1 α was shown stabilized by IHC in OS-93^{ND1}-derived xenografts, and this was confirmed also by a lower α KG/SA ratio and by down-regulation of its responsive genes (LDHA, VEGF, GLUT1). In addition, we showed that allotopic expression of ND1 was preserved also in cell lines isolated from OS-93^{ND1}-derived xenografts, such as its incorporation in a functioning complex I.

Taken together, these results provide unambiguous and further evidence about the role of complex I in the tumorigenesis process, due to its close relation with HIF, which is considered one of the master regulators of the metabolic adaptation needed for cancer cells to progress to malignancy. Furthermore, a few important implications stem from

these results, concerning some possible clinical applications, arising, for example, from the translation of a genetic into a metabolic shift of the α -KG/SA ratio toward α -KG, which supports the use of cell-permeable α -KG derivatives in anticancer therapy (MacKenzie et al., 2007). Other strategies may impinge on induction of complex I disassembly in patients not harboring mtDNA mutations, degradation of assembly factors, or even modulation of mitochondrial biogenesis to induce both the mutation and its accumulation. Moreover, induction of oncocytic transformation could be envisioned as an approach to reduce tumor growth and abolish aggressive and metastatic potential. Our hope is that the results achieved in this study from allotopic strategy and its *in vivo* applications, can open new effective perspectives on clinical therapy of diseases caused by mtDNA mutations, both degenerative diseases and tumors.

References

Abrahams JP, Leslie AG, Lutter R, et al. Structure at 2.8 Å resolution of F₁-ATPase from bovine heart mitochondria. *Nature*. 1994; 370:621-628.

Ambrosini-Spaltro A, Salvi F, Betts C-M, Frezza G-P, Piemontese A, Del Prete P, Baldoni C, Foschini M-P, Viale G. *Virchows Arch*. 2006; 448: 442-448.

Anderson S, Bankier AT, Barrell BG, et al. Sequence and organization of the human mitochondrial genome. *Nature*. 1981; 290:457-465.

Andreu AL, Bruno C, Shanske S, et al. Missense mutation in the mtDNA cytochrome b gene in a patient with myopathy. *Neurology*. 1998; 51:1444–1447.

Andreu AL, Bruno C, Dunne TC, et al. 1999a. A nonsense mutation (G15059A) in the cytochrome b gene in a patient with exercise intolerance and myoglobinuria. *Ann Neurol*. 1999a ; 45:127–130.

Andreu AL, Hanna MG, Reichmann H, et al. Exercise intolerance due to mutations in the cytochrome b gene of mitochondrial DNA. *N Engl J Med*. 1999b;341:1037–1044.

Bartlett K, Eaton S. Mitochondrial beta-oxidation. *Eur J Biochem*. 2004; 271:462 – 469.

Baysal BE, Ferrell RE, Willett-Brozick JE, et al. Mutations in SDHD, a mitochondrial complex II gene, in hereditary paraganglioma. *Science*. 2000; 287:848-851

Belevich I, Verkhovsky MI, Wikstrom M. Proton-coupled electron transfer drives the proton pump of cytochrome c oxidase. *Nature*. 2006; 440: 829–832.

Berry EA, Guergova-Kuras M, Huang LS, et al. Structure and function of cytochrome bc complexes. *Annu Rev Biochem*. 2000; 69:1005-1075.

Bleeker FE, Lamba S, Leenstra S, et al. IDH1 mutations at residue p.R132 (IDH1^{R132}) occur frequently in high-grade gliomas but not in other solid tumors. *Hum Mutat*. 2009; 30:7-11.

Boekema EJ, Braun HP. Supramolecular structure of the mitochondrial oxidative phosphorylation system. *J Biol Chem*. 2008; 283:20612.

- Bonnefont JP, Djouadi F, Prip-Buus C, et al. Carnitine palmitoyltransferases 1 and 2: biochemical, molecular and medical aspects. *Mol Aspects Med.* 2004; 25:495 – 520.
- Bonnet C, Augustin S, Ellouze S, et al. The optimized allotropic expression of ND1 or ND4 genes restores respiratory chain complex I activity in fibroblast harboring mutations in these genes. *Biochim Biophys Acta.* 2008; 1783: 1707-1717.
- Bonnet C, Kaltimbacher V, Ellouze S, et al. Allotropic mRNA localization to the mitochondrial surface rescue respiratory chain defects in fibroblast harboring mitochondrial DNA mutations affecting complex I or V subunits. *Rejuvenation Res.* 2007; 10: 127-144.
- Boulton J, Fidler C, Mills KI, et al. Amplification of mitochondrial DNA in acute myeloid leukaemia. *Br J Haematol.* 1996; 95: 426–431.
- Bourges I, Ramus C, Mousson de Camaret B, et al. Structural organization of mitochondrial human complex I: role of the ND4 and ND5 mitochondria-encoded subunits and interaction with prohibitin. *Biochem J.* 2004; 383:491–499.
- Bradford MM. A rapid and sensitive method for the quantitation of microgram quantities of protein utilizing the principle of protein-dye binding. *Anal Biochem.* 1976; 72:248-254.
- Brandon M, Baldi P, Wallace DC.. Mitochondrial mutations in cancer. *Oncogene.* 2006; 25:4647–4662.
- Brière JJ, Favier J, Gimenez-Roqueplo AP, and Rustin P. Tricarboxylic acid cycle dysfunction as a cause of human diseases and tumor formation. *Am J Physiol Cell.* 2006; 291: C1114-1120
- Brown MD, Torroni A, Reckord CL, Wallace DC. Phylogenetic analysis of Leber's hereditary optic neuropathy mitochondrial DNA's indicates multiple independent occurrences of the common mutations. *Hum Mutat.* 1995; 6:311–325.

Brown MD, Starikovskaya E, Derbeneva O, et al. The role of mtDNA background in disease expression: A new primary LHON mutation associated with Western Eurasian haplogroup J. *Hum Genet.* 2002; 110:130–138.

Brown MD, Sun F, Wallace DC.. Clustering of Caucasian Leber hereditary optic neuropathy patients containing the 11778 or 14484 mutations on an mtDNA lineage. *Am J Hum Genet.* 1997; 60:381-387.

Calvaruso MA, Smeitink J, Nijtmans L. Electrophoresis techniques to investigate defects in oxidative phosphorylation. *Methods.* 2008; 46: 281-287.

Capaldi RA, Aggeler R. Mechanism of the $F_{(1)}F_{(0)}$ -type ATP synthase, a biological rotarymotor. *Trends Biochem Sci.* 2002; 27:154-60.

Capaldi RA, Sweetland J, Merli A. Polypeptides in the succinate-coenzyme Q reductase segment of the respiratory chain. *Biochemistry.* 1977 Dec 27;16(26):5707-10.

Carelli V, Baracca A, Bargi S, et al. Biochemical-clinical correlation in patients with different loads of the mitochondrial DNA T8993G mutation. *Arch Neurol.* 2002; 59: 264-270.

Carroll AJ, Baer MR, Caligiuri MA, et al. IDH1 and IDH2 gene mutations identify novel molecular subsets within de novo cytogenetically normal acute myeloid leukemia: a Cancer and Leukemia Group B study. *J Clin Oncol.* 2010; 28:2348-2355.

Carroll J, Fearnley IM, Shannon RJ, et al. Analysis of the subunit composition of complex I from bovine heart mitochondria. *Mol Cell Proteomics,* 2003; 2: 117-126.

Carroll J, Fearnley IM, Skehel JM, Shannon RJ, Hirst J, Walker JE. Bovine complex I is a complex of 45 different subunits. *J Biol Chem.* 2006; 281:32724-7.

Carroll J, Shannon RJ, Fearnley IM, et al. Definition of the nuclear encoded protein composition of bovine heart mitochondrial complex I. Identification of two new subunits. *J Biol Chem.* 2002; 277:50311-50317.

Carozzo R, Dionisi-Vici C, Steuerwald U, et al. SUCLA2 mutations are associated with mild methylmalonic aciduria, Leigh-like encephalomyopathy, dystonia and deafness. *Brain*. 2007; 130(Pt 3):862–874.

Carvajal-Carmona LG, Alam NA, Pollard PJ, et al. Adult leydig cell tumors of the testis caused by germline fumarate hydratase mutations. *J Clin Endocrinol Metab*. 2006; 91:3071-3075.

Cervera AM, Bayley JP, Devilee P, McCreath KJ. Inhibition of succinate dehydrogenase dysregulates histone modification in mammalian cells. *Mol Cancer*. 2009; 8:89.

Chan SS, Copeland WC. DNA polymerase gamma and mitochondrial disease: understanding the consequence of POLG mutations. *Biochim Biophys Acta*. 2009; 1787; 312-319.

Chatterjee A, Mambo E, Sidransky D. Mitochondrial DNA mutations in human cancer. *Oncogene*. 2006; 25: 4663–4674.

Chen H, Chan DC. Mitochondrial dynamics in mammals. *Curr Top Dev Biol*. 2004; 59:119-44.

Chen H, SA Detmer, et al. Mitofusins Mfn1 and Mfn2 coordinately regulate mitochondrial fusion and are essential for embryonic development. *J Cell Biol*. 2003; 160:189-200.

ChenY, Cairns R, Papandreou I, et al. Oxygen consumption can regulate the growth of tumors, a new perspective on the Warburg effect. *Plos One*. 2009; 4: e7033.

Clayton DA. Vertebrate mitochondrial DNA: a circle of surprises. *Exp Cell Res*. 2000; 255:4–9.

Costa-Guda J, Tokura T, Roth SI, Arnold A. Mitochondrial DNA mutations in oxyphilic and chief cell parathyroid adenomas. *BMC Endocr Disord*. 2007; 7:8.

D'Herde K, De Prest B, Mussche S, et al. Ultrastructural localization of cytochrome c in apoptosis demonstrates mitochondrial heterogeneity. *Cell Death. Differ.* 2001; 7:331-337.

Dang L, White DW, Gross S, Bennett BD, et al. Cancer-associated IDH1 mutations produce 2-hydroxyglutarate. *Nature.* 2009; 462:739-744.

Darrouzet E, Moser CC, Dutton PL, Daldal F. Large scale domain movement in cytochrome bc(1): a new device for electron transfer in proteins. *Trends Biochem Sci.* 2001; 26:445-51.

De Benedictis G, Rose G, Carrieri G, et al. Mitochondrial DNA inherited variants are associated with successful aging and longevity in humans. *FASEB J.* 1999; 13:1532-1536.

Delettre C, Lenaers G, Griffoin JM, 2000. Nuclear gene OPA1, encoding a mitochondrial dynamin-related protein, is mutated in dominant optic atrophy. *Nat Genet* 26:207-210.

DiMauro S, Mancuso M. Mitochondrial diseases: Therapeutic approaches. *Biosci Rep.* 2007; 27: 125-137.

Efremov RG, Baradaran R, Sazanov LA. The architecture of respiratory complex I, *Nature.* 2010; 465: 441-445.

Falkenberg M, Larsson NG, Gustafsson CM. DNA replication and transcription in mammalian mitochondria. *Annu Rev Biochem.* 2007; 76:679-699.

Faxen K, Gilderson G, Adelroth P, Brzezinski P. A mechanistic principle for proton pumping by cytochrome c oxidase. *Nature.* 2005; 437: 286-289.

Fernandez-Silva P, Enriquez JA & Montoya J. Replication and transcription of mammalian mitochondrial DNA. *Exp Physiol.* 2003; 88: 41-56.

Fliss MS, Usadel H, Caballero OL, et al. Facile detection of mitochondrial DNA mutations in tumors and bodily fluids. *Science.* 2000; 287: 2017-2019.

Frey TG and Mannella CA. The internal structure of mitochondria. *Trends. Biochem. Sci.* 2000; 25, 319-324.

Frey TG, Renken CW, Perkins GA. Insight into mitochondrial structure and function from electron tomography. *Biochim Biophys Acta.* 2002; 1555:196-203.

Frezza C, Tennant DA, Gottlieb E. IDH1 mutations in gliomas: when an enzyme loses its grip. *Cancer Cell.* 2010; 17:7-9.

Friedrich T, Bottcher B. The gross structure of the respiratory complex I: a Lego system. *Biochim Biophys Acta.* 2004; 1608: 1–9.

Gasparre G, Bonora E, Tallini G, Romeo G. Molecular features of thyroid oncocyctic tumors. *Mol Cell Endocrinol.* 2010; 321:67 – 76.

Gasparre G, Romeo G, Rugolo M, Porcelli AM. Learning from oncocyctic tumors: why choose inefficient mitochondria? *Biochim Biophys Acta.* 2011; 1807: 633-642.

Gasparre G, Hervouet E, et al. Clonal expansion of mutated mitochondrial DNA is associated with tumor formation and complex I deficiency in the benign renal oncocytoma. *Hum Mol Genet.* 2008; 17:986 – 95.

Gasparre G, Iommarini L, Porcelli AM, et al. An inherited mitochondrial DNA disruptive mutation shifts to homoplasmy in oncocyctic tumor cells. *Hum Mutat.* 2009; 30: 391 – 6.

Gasparre G, Kurelac I, Capristo M, et al. A mutation threshold distinguishes the antitumorigenic effect of the mitochondrial gene MND1, an Oncojanus function. *Cancer Res.* 2011; 71(19): 6220-6229.

Gasparre G, Porcelli AM, Bonora E, et al. Disruptive mitochondrial DNA mutations in complex I subunits are markers of oncocyctic phenotype in thyroid tumors. *PNAS.* 2007; 104(21): 9001-6.

Gasparre G, Romeo G, Rugolo M, Porcelli AM. Learning from oncocyctic tumors: why choose inefficient mitochondria? *Biochim Biophys Acta.* 2011b; 1807:633-42.

Gershoni M, Fuchs A, Shani N, et al. Coevolution predicts direct interactions between mtDNA-encoded and nDNA-encoded subunits of oxidative phosphorylation complex I. *J Mol Biol.* 2010; 404: 158–171.

Ghelli A, Porcelli AM, Zanna C, et al. The Background of Mitochondrial DNA Haplogroup J Increases the Sensitivity of Leber's Hereditary Optic Neuropathy Cells to 2,5-Hexanedione Toxicity. *Plos One.* 2009; 4(11): e7922.

Gong LB, Luo XL, Liu SY, et al. Correlations of GRIM-19 and its target gene product STAT3 to malignancy of human colorectal carcinoma. *Ai Zheng.* 2007; 26: 683-687.

Goto Y, Nonaka I, Horai S. A mutation in the tRNA^{Leu(UUR)} gene associated with the MELAS subgroup of mitochondrial encephalomyopathies. *Nature.* 1990; 348:651–653.

Gottlieb E, Tomlinson IP. Mitochondrial tumour suppressors: a genetic and biochemical update. *Nat Rev Cancer.* 2005; 5:857-866.

Gray RE, Law RH, Devenish RJ, Nagley P. Allotopic expression of mitochondrial ATP synthase genes in nucleus of *Saccharomyces cerevisiae*. *Methods Enzymol.* 1996; 264: 369-89.

Guenebaut V, Schlitt A, Weiss H, et al. Consistent structure between bacterial and mitochondrial NADH:ubiquinone oxidoreductase (complex I). *J. Mol. Biol.* 1998; 276: 105–112.

Guy J, Qi X, Pallotti F, Schon EA, et al. Rescue of a mitochondrial deficiency causing Leber Hereditary Optic Neuropathy. *Ann Neurol.* 2002; 52(5): 534-42.

Hendrickson SL, Hutcheson HB, Ruiz-Pesini E, et al. Mitochondrial DNA haplogroups influence AIDS progression. *AIDS.* 2008; 22:2429–2439.

Hewitson KS, Lienard BM, McDonough MA, et al. Structural and mechanistic studies on the inhibition of the hypoxia-inducible transcription factor hydroxylases by tricarboxylic acid cycle intermediates. *J Biol Chem.* 2007; 282:3293-3301.

Hirst J, Carroll J, Fearnley IM, et al. The nuclear encoded subunits of complex I from bovine heart mitochondria. *Biochim Biophys Acta*. 2003; 1604: 135–150.

Hoefs SJ, Dieteren CE, Rodenburg RJ, et al. Baculovirus complementation restores a novel NDUFAF2 mutation causing complex I deficiency. *Hum. Mutat*. 2009; 30: E728–E736.

Holt IJ, Harding AE, Petty RK, Morgan-Hughes JA. A new mitochondrial disease associated with mitochondrial DNA heteroplasmy. *Am J Hum Genet*. 1990; 46:428–433.

Holt IJ, Harding AE, Morgan-Hughes JA.. Deletions of muscle mitochondrial DNA in patients with mitochondrial myopathies. *Nature*. 1988; 331:717–719.

Hoogenraad NJ, Ward LA, Ryan MT. Import and assembly of proteins into mitochondria of mammalian cells. *Biochim Biophys Acta*. 2002; 1592: 97–105.

Housley SL, Lindsay RS, Young B, et al. Renal carcinoma with giant mitochondria associated with germ-line mutation and somatic loss of the succinate dehydrogenase B gene. *Histopathology*. 2010; 56: 405-40.

Houten SM, and Wanders R JA. A general introduction to the biochemistry of mitochondrial fatty acid β -oxidation. *J Inherit Metab Dis*. 2010; 33:469-477.

Hunte C, Zickermann V, Brandt U. Functional modules and structural basis of conformational coupling in mitochondrial complex I. *Science*. 2010; 329: 448–451.

Isaacs JS, Jung YJ, Mole DR, et al. HIF overexpression correlates with biallelic loss of fumarate hydratase in renal cancer: novel role of fumarate in regulation of HIF stability. *Cancer Cell*. 2005; 8:143-153

Ishikawa K, Takenaga K, Akimoto M, et al. ROS-generating mitochondrial DNA mutations can regulate tumor cell metastasis. *Science*. 2008; 320:661–664.

Ivanova R, Lepage V, Charron D, Schachter F. Mitochondrial genotype associated with French Caucasian centenarians. *Gerontology*. 1998; 44:349.

- Janssen RJ, Nijtmans LG, van den Heuvel LP, Smeitink JA. Mitochondrial complex I: structure, function and pathology, *J. Inherit. Metab. Dis.* 2006; 29: 499–515.
- Kalakonda S, Nallar SC, Lindner DJ, et al. Tumor-suppressive activity of the cell death activator GRIM-19 on a constitutively active signal transducer and activator of transcription 3. *Cancer Res.* 2007; 67: 6212–6220.
- Kapsa R, Thompson GN, Thorburn DR, et al. A novel mtDNA deletion in an infant with Pearson syndrome. *J Inherit Metab Dis.* 1994; 17:521–526.
- Kaukonen J, Juselius JK, Tiranti V, et al. Role of adenine nucleotide translocator 1 in mtDNA maintenance. *Science.* 2000; 289:782–785.
- Khusnutdinova E, Gilyazova I, Ruiz-Pesini E, et al, A mitochondrial etiology of neurodegenerative diseases: Evidence from Parkinson's disease. *Ann N Y Acad Sci.* 2008; 1147:1–20.
- Krause F, Reifschneider NH, Vocke D, et al. "Respirasome"-like supercomplexes in green leaf mitochondria of spinach. *J Biol Chem.* 2004 ; 279:48369-75.
- Krebs H and Johnson WA. The role of citric acid in intermediate metabolism in animal tissues. *Enzymologia.* 1937; 4: 148 –156.
- Kujoth GC, Hiona A, Pugh TD, et al. Mitochondrial DNA mutations, oxidative stress, and apoptosis in mammalian aging. *Science.* 2005; 309:481–484.
- Kurelac I, Lang M, Zuntini R, et al. Searching for a needle in the haystack: comparing six methods to evaluate heteroplasmy in difficult sequence context. *Biotech Adv.* 2011; 30(1): 363-71.
- Kwong JQ, Henning MS, Starkov AA, Manfredi G. The mitochondrial respiratory chain is a modulator of apoptosis. *J Cell Biol.* 2007; 179: 1163-1177.
- Laloi-Michelin M, Meas T, Ambonville C, et al. The clinical variability of maternally inherited diabetes and deafness (Midd) is associated with the degree of heteroplasmy in blood leukocytes. *J Clin Endocrinol Metab.* 2009; 94(8): 3025-3030.

- Lancaster CR, Kröger A. Succinate:quinone oxidoreductases: new insights from X-ray crystal structures. *Biochim Biophys Acta*. 2000; 1459:422-31.
- Launonen V, Vierimaa O, Kiuru M, et al. Inherited susceptibility to uterine leiomyomas and renal cell cancer. *Proc Natl Acad Sci USA*: 2001; 98: 3387-3392.
- Lazarou M, McKenzie M, Ohtake A, et al. Analysis of the assembly profiles for mitochondrial- and nuclear-DNA-encoded subunits into complex I. *Mol Cell Biol*. 2007; 27: 4228–4237.
- Lazarou M, Thorburn DR, Ryan MT, McKenzie M. Assembly of mitochondrial complex I and defects in disease. *Biochim Biophys Acta*. 2009; 1793: 78–88.
- Lee MS, Yuet-Wa JC, Kong SK. Effects of polyphyllin D, a steroidal saponin in *Paris polyphylla*, in growth inhibition of human breast cancer cells and in xenograft. *Cancer Biol Ther*. 2005; 4: 1248–1254.
- Lehtonen HJ, Kiuru M, Ylisaukko-Oja SK, et al. Increased risk of cancer in patients with fumarate hydratase germline mutation. *J Med Genet*. 2006; 43:523-526.
- Lemarie A, and Grimm S. Mitochondrial respiratory chain complexes: apoptosis sensors mutated in cancer. *Oncogene*. 2011; 30: 3985-4003.
- Liu X, Weaver D, Shirihai O, Hajnóczky G. Mitochondrial 'kiss-and-run': interplay between mitochondrial motility and fusion-fission dynamics. *EMBO J*. 2009; 28:3074-89.
- Lu J, Sharma LK, Bai Y. Implications of mitochondrial DNA mutations and mitochondrial dysfunction in tumorigenesis. *Cell Res*. 2009;19: 802–815.
- MacKenzie ED, Selak MA, Tennant DA, et al. Cell-permeating alpha-ketoglutarate derivatives alleviate pseudohypoxia in succinate dehydrogenase-deficient cells. *Mol Cell Biol*. 2007; 27:3282-3289.
- Mambo E, Chatterjee A, Xing M, et al. Tumor-specific changes in mtDNA content in human cancer. *Int J Cancer*. 2005; 116: 920–924.

Mandel H, Szargel R, Labay V, et al. The deoxyguanosine kinase gene is mutated in individuals with depleted hepatocerebral mitochondrial DNA. *Nat Genet.* 2001; 29:337–341.

Manfredi G, Fu J, Ojaimi J, Sadlock JE, et al. Rescue of deficiency in ATP synthesis by transfer of MTATP6, a mitochondrial DNA-encoded gene, to the nucleus. *Nat Genet.* 2002; 30(4):394-9.

Manfredi G, Yang L, Gajewski CD, et al. Measurements of ATP in mammalian cells. *Methods.* 2002b; 26: 317-326.

Mannella CA, Marko M, Buttle K. Reconsidering mitochondrial structure: new views of an old organelle. *Trends Biochem Sci.* 1997; 22:37-8.

Mannella CA, Marko M, Penczek P, Barnard D, Frank J. The internal compartmentation of rat-liver mitochondria: tomographic study using the high-voltage transmission electron microscope. *Microsc Res Tech.* 1994; 27:278-83.

Mao CC and Holt IJ. Clinical and molecular aspects of diseases of mitochondrial DNA instability. *Chang Gung Med J.* 2009; 32:354-69.

Mathiesen C, Hagerhall C. Transmembrane topology of the NuoL, M and N subunits of NADH:quinone oxidoreductase and their homologues among membrane-bound hydrogenases and bona fide antiporters. *Biochim Biophys Acta.* 2002; 1556: 121–132.

Mayr JA, Meierhofer D, Zimmermann F, et al. Loss of complex I due to mitochondrial DNA mutations in renal oncocytoma. *Clin Cancer Res.* 2008; 14:2270-5.

Maximo V, Lima J, Soares P. et al. GRIM-19 in health and disease. *Adv Anat Pathol.* 2008; 15: 46–53.

Mimaki M, Wang X, McKenzie M. Understanding mitochondrial complex I assembly in health and disease. *Biochim Biophys Acta.* 2011.

MITOMAP: A human mitochondrial Genome Database. (Available from : <http://www.mitomap.org>)

Mishmar D, Ruiz-Pesini EE, Golik P, et al. Natural selection shaped regional mtDNA variation in humans. *Proc Natl Acad Sci USA*. 2003; 100:171–176.

Mita S, Schmidt B, Schon EA, et al. Detection of ‘deleted’ mitochondrial genomes in cytochrome-c oxidase-deficient muscle fibers of a patient with Kearns–Sayre syndrome. *Proc Natl Acad Sci USA*. 1989; 86:9509–9513.

Mokranjac D, and Neupert W. Protein import into mitochondria. *Biochem Soc Trans*. 2005; 33: 1019- 1023.

Moro L, Arbini AA, Marra E, Greco M. Mitochondrial DNA depletion reduces PARP-1 levels and promotes progression of the neoplastic phenotype in prostate carcinoma, *Cell Oncol*. 2008; 30: 307–322.

Nachman MW, Brown WM, Stoneking M, Aquadro CF. Nonneutral mitochondrial DNA variation in humans and chimpanzees. *Genetics*. 1996; 142:953–963.

Nass MM. The circularity of mitochondrial DNA. *Proc Natl Acad Sci USA*. 1966; 56: 1215-1222.

Nicholls, DG, and Ferguson SJ, *Bioenergetics 3* Academic Press, London, 2002.

Nishino I, Spinazzola A, Hirano M. Thymidine phosphorylase gene mutations in MNGIE, a human mitochondrial disorder. *Science*. 1999; 283:689–692.

Oca-Cossio J, Kenyon L, Hao H, Moraes CT. Limitations of allotopic expression of mitochondrial genes in mammalian cells. *Genetics*. 2003; 165(2): 707-20.

Palmieri L, Alberio S, Pisano I, et al. Complete loss-of-function of the heart/muscle-specific adenine nucleotide translocator is associated with mitochondrial myopathy and cardiomyopathy. *Hum Mol Genet*. 2005; 14:3079–3088.

Park CB, Larsson NG. Mitochondrial DNA mutations in disease and aging. *J Cell Biol*. 2011; 193(5) :809-18.

Park JS, Sharma LK, Li H, et al. A heteroplasmic, not homoplasmic, mitochondrial DNA mutation promotes tumorigenesis via alteration in reactive oxygen species generation and apoptosis. *Hum Mol Genet.* 2009; 18: 1578-89.

Parsons DW, Jones S, Zhang X, et al. An integrated genomic analysis of human glioblastoma multiforme. *Science.* 2008; 321:1807-1812.

Perales-Clemente E, Fernandez-Silva P, Acin-Perez R, Perez-Martos A, Enriquez JA. Allotopic expression of mitochondrial-encoded genes in mammals: achieved goal, undemonstrated mechanism or impossible task? *Nucleic Acids Res.* 2011; 39(1): 225-34.

Perales-Clemente E, Fernandez-Vizarra E, Acin-Perez R, et al. Five entry points of the mitochondrially encoded subunits in mammalian complex I assembly. *Mol Cell Biol.* 2010; 30: 3038–3047.

Perkins G, Renken C, Martone ME, Young SJ, Ellisman M, Frey T. Electron tomography of neuronal mitochondria: three-dimensional structure and organization of cristae and membrane contacts. *J Struct Biol.* 1997; Aug;119(3): 260-72.

Perotti ME, Anderson WA, and Swift H. Quantitative cytochemistry of the diaminobenzidine cytochrome oxidase reaction product in mitochondria of cardiac muscle and pancreas. *J. Histochem. Cytochem.* 1983; 31:351-365.

Petros JA, Baumann AK, Ruiz-Pesini E, et al. mtDNA mutations increase tumorigenicity in prostate cancer. *Proc Natl Acad Sci USA.* 2005; 102:719–724.

Pollard PJ, Briere JJ, Alam NA, et al. Accumulation of Krebs cycle intermediates and over-expression of HIF1alpha in tumours which result from germline FH and SDH mutations. *Hum Mol Genet.* 2005; 14:2231-2239.

Polyak K, Li Y, Zhu H, et al. Somatic mutations of the mitochondrial genome in human colorectal tumours. *Nat Genet.* 1998; 20: 291–293.

- Porcelli AM, Ghelli A, Ceccarelli C, et al. The genetic and metabolic signature of oncogenic transformation implicates HIF1 α destabilization. *Hum Mol Gen.* 2010; 19(6): 1019-1032.
- Potluri P, Yadava N, Scheffler IE. The role of the ESSS protein in the assembly of a functional and stable mammalian mitochondrial complex I (NADH-ubiquinone oxidoreductase). *Eur J Biochem.* 2004; 271: 3265–3273.
- Procaccio V, Wallace DC. Late-onset Leigh syndrome in a patient with mitochondrial complex I NDUFS8 mutations. *Neurology.* 2004; 62:1899–1901.
- Ramsay RR, Gandour RD, van der Leij FR. Molecular enzymology of carnitine transfer and transport. *Biochim Biophys Acta.* 2001; 1546:21-43.
- Ricketts C, Woodward ER, Killick P, et al. Germline SDHB mutations and familial renal cell carcinoma. *J Natl Cancer Inst.* 2008; 100:1260-1262.
- Rose G, Passarino G, Carrieri G, et al. Paradoxes in longevity: Sequence analysis of mtDNA haplogroup J in centenarians. *Eur J Hum Genet.* 2001; 9:701–707.
- Ruiz-Pesini E, Wallace DC. Evidence for adaptive selection acting on the tRNA and rRNA genes of the human mitochondrial DNA. *Hum Mutat.* 2006; 27:1072–1081.
- Ruiz-Pesini E, Mishmar D, Brandon M, et al. Effects of purifying and adaptive selection on regional variation in human mtDNA. *Science.* 2004; 303:223–226.
- Rustin P, Rotig A. Inborn errors of complex II-unusual human mitochondrial diseases. *Biochim Biophys Acta.* 2002; 1553:117-122.
- Saada A, Shaag A, Mandel H, Nevo Y, Eriksson S, Elpeleg O. Mutant mitochondrial thymidine kinase in mitochondrial DNA depletion myopathy. *Nat Genet.* 2001; 29:342–344.
- Saada A, Vogel RO, Hoefs SJ, et al. Mutations in NDUFAF3 (C3ORF60), encoding an NDUFAF4 (C6ORF66)-interacting complex I assembly protein, cause fatal neonatal mitochondrial disease. *Am J Hum Genet.* 2009; 84: 718–727

- Saraste M. Oxidative phosphorylation at the fin de siècle. *Science*. 1999; 283:1488-93.
- Sazanov LA, Carroll J, Holt P, et al. A role for native lipids in the stabilization and two-dimensional crystallization of the *Escherichia coli* NADH-ubiquinone oxidoreductase (complex I). *J Biol Chem*. 2003; 278: 19483–19491.
- Sazanov LA, Hinchliffe P. Structure of the hydrophilic domain of respiratory complex I from *Thermus thermophilus*. *Science*. 2006; 311: 1430–1436.
- Sazanov LA, Peak-Chew SY, Fearnley IM, Walker JE. Resolution of the membrane domain of bovine complex I into subcomplexes : implications for the structural organization of the enzyme. *Byochemistry*. 2000; 39: 7229-7235.
- Scarpulla RC. Transcriptional paradigms in mammalian mitochondrial biogenesis and function. *Physiol Rev*. 2008; 88:611-638.
- Schäfer E, Seelert H, Reifschneider NH, et al. Architecture of active mammalian respiratory chain supercomplexes. *J Biol Chem*. 2006; 281:15370-5.
- Schägger H and Pfeiffer K. Supercomplexes in the respiratory chains of yeast and mammalian mitochondria. *EMBO J*. 2000; 19:1777-83.
- Scheffler IE, Yadava N, Potluri P. Molecular genetics of complex I-deficient Chinese hamster cell lines. *Biochim Biophys Acta*. 2004; 1659: 160–171.
- Schofield CJ, Ratcliffe PJ. Oxygen sensing by HIF hydroxylases. *Nat Rev Mol Cell Biol*. 2004; 5:343-354.
- Schultz BE, Chans SI. Structures and proton-pumping strategies of mitochondrial respiratory enzymes. *Annu Rev Biophys Biomol Struct*. 2001; 30: 23-65.
- Schriner SE, Ogburn CE, Smith AC, et al. Levels of DNA damage are unaltered in mice overexpressing human catalase in nuclei. *Free Radic Biol Med*. 2000; 29:664–673.
- Schriner SE, Linford NJ, Martin GM, et al. Extension of murine life span by overexpression of catalase targeted to mitochondria. *Science*. 2005; 308:1909–1911.

Scott RA, Wilson RH, Goodwin WH, et al. Mitochondrial DNA lineages of elite Ethiopian athletes. *Comp Biochem Physiol B Biochem Mol Biol.* 2005; 140:497–503.

Scott RA, Fuku N, Onywera VO, et al. Mitochondrial haplogroups associated with elite Kenyan athlete status. *Med Sci Sports Exerc.* 2009; 41:123–128.

Selak MA, Armour SM, MacKenzie ED, et al. Succinate links TCA cycle dysfunction to oncogenesis by inhibiting HIF- α prolyl hydroxylase. *Cancer Cell.* 2005; 7:77-85

Selvanayagam P, Rajaraman S. Detection of mitochondrial genome depletion by a novel cDNA in renal cell carcinoma. *Lab Invest.* 1996; 74:592–599.

Shidara Y, Yamagata K, Kanamori T, et al. Positive contribution of pathogenic mutations in the mitochondrial genome to the promotion of cancer by prevention from apoptosis. *Cancer Res.* 2005; 65: 1655–1663.

Shoffner JM, Lott MT, Lezza AM, et al. Myoclonic epilepsy and ragged-red fiber disease (MERRF) is associated with a mitochondrial DNA tRNA^{Lys} mutation. *Cell.* 1990; 61:931–937.

Shoffner JM, Brown MD, Torroni A, et al. Mitochondrial DNA variants observed in Alzheimer disease and Parkinson disease patients. *Genomics.* 1993; 17:171–184.

Simonnet H, Alazard N, Pfeiffer K, et al. Low mitochondrial respiratory chain content correlates with tumor aggressiveness in renal cell carcinoma. *Carcinogenesis.* 2002; 23: 759–768.

Singh KK, Ayyasamy V, Owens KM, et al. Mutations in mitochondrial DNA polymerase-gamma promote breast tumorigenesis. *J Hum Genet.* 2009a; 54: 516–524.

Singh KK, Kulawiec M. Mitochondrial DNA polymorphism and risk of cancer. *Methods Mol Biol.* 2009b; 471: 291–303.

Spelbrink JN, Li FY, Tiranti V, et al. Human mitochondrial DNA deletions associated with mutations in the gene encoding Twinkle, a phage T7 gene 4-like protein localized in mitochondria. *Nat Genet.* 2001; 28:223–231.

Stojanovski D, Johnston AJ, Streimann I, et al. Import of nuclear-encoded proteins into mitochondria. *Exp Physiol.* 2003; 88: 57–64.

Stratakis CA, Carney JA. The triad of paragangliomas, gastric stromal tumours and pulmonary chondromas (Carney triad), and the dyad of paragangliomas and gastric stromal sarcomas (Carney – Stratakis syndrome): molecular genetics and clinical implications. *J Intern Med.* 2009; 266:43-52.

Sugiana C, Pagliarini DJ, McKenzie M, et al. Mutation of C20orf7 disrupts complex I assembly and causes lethal neonatal mitochondrial disease. *Am Hum Genet.* 2008; 83: 468–478.

Sylvestre J, Margeot A, Jacq C, et al. The role of 3'UTR in mRNA sorting to the vicinity of mitochondria is conserved from yeast to human cells. *Mol Biol Cell.* 2003; 14: 3848-3856.

Szklarczyk R, Wanschers BF, Nabuurs SB, et al. NDUFB7 and NDUFA8 are located at the intermembrane surface of complex I. *FEBS Lett.* 2011; 585:737–743.

Taylor RW, and Turnbull DM. Mitochondrial DNA mutations in human diseases. *Nat Rev Genet.* 2005; 6: 389-402.

Tomlinson IP, Alam NA, Rowan AJ, et al. Germline mutations in FH predispose to dominantly inherited uterine fibroids, skin leiomyomata and papillary renal cell cancer. *Nat Genet.* 2002; 30: 406-410.

Torrioni A, Petrozzi M, D'Urbano L, et al. Haplotype and phylogenetic analyses suggest that one European-specific mtDNA background plays a role in the expression of Leber hereditary optic neuropathy by increasing the penetrance of the primary mutations 11778 and 14484. *Am J Hum Genet.* 1997; 60:1107–1121.

Trifunovic A. Mitochondrial DNA and ageing. *Biochim Biophys Acta*. 2006; 1757:611-7.

Trifunovic A, Wredenberg A, Falkenberg M, et al. Premature ageing in mice expressing defective mitochondrial DNA polymerase. *Nature*. 2004; 429:417–423.

Trounce IA, Kim YL, Jun AS, et al. Assessment of mitochondrial oxidative phosphorylation in patient muscle biopsies, lymphoblasts, and transmitochondrial cell lines. *Methods Enzymol*. 1996; 264:484-509.

Tuschen G, Sackmann U, Nehls U, et al. Assembly of NADH:ubiquinone reductase (complex I) in *Neurospora* mitochondria. Independent pathways of nuclear-encoded and mitochondrially encoded subunits. *J Mol Biol*. 1990; 213: 845–857.

Tseng LM, Yin PH, Chi CW. Mitochondrial DNA mutations and mitochondrial DNA depletion in breast cancer. *Genes Chromosom Cancer*. 2006; 45: 629–638.

van der Leij FR, Huijkman NC, Boomsma C, et al. Genomics of the human carnitine acyltransferase genes. *Mol Genet Metab*. 2000; 71:139 – 153

Van Goethem G, Dermaut B, Lofgren A, et al. Mutation of POLG is associated with progressive external ophthalmoplegia characterized by mtDNA deletions. *Nat Genet*. 2001; 28:211–212.

van Nederveen FH, Korpershoek E, Lenders JW, et al. Somatic SDHB mutation in an extraadrenal pheochromocytoma. *N Engl J Med*. 2007; 357:306-308.

Vogel F, Bornhövd C, Neupert W, Reichert AS. Dynamic subcompartmentalization of the mitochondrial inner membrane. *J Cell Biol*. 2006; 175:237-47.

Vogel RO, Smeitink JA, Nijtmans LG. Human mitochondrial complex I assembly: a dynamic and versatile process. *Biochim Biophys Acta*. 2007; 1767: 1215–1227.

Vonck J, Schäfer E. Supramolecular organization of protein complexes in the mitochondrial inner membrane. *Biochim Biophys Acta*. 2009; 1793:117-24.

Walker JE. The NADH:ubiquinone oxidoreductase (complex I) of respiratory chains. *Q Rev Biophys.* 1992; 25:253-324.

Wallace DC. Mitochondria and Cancer: Warburg Address. *Cold Spring Harb Symp Quant Biol.* 2005a; 70:363–374.

Wallace DC. A mitochondrial paradigm of metabolic and degenerative diseases, aging, and cancer: A dawn for evolutionary medicine. *Annu Rev Genet.* 2005c; 39:359–407.

Wallace DC, Fan W, Procaccio V. Mitochondrial energetics and therapeutics. *Annu Rev Pathol.* 2010; 5:297–348.

Wallace DC, Lott MT. Mitochondrial genes in degenerative diseases, cancer and aging. 2002. In: Rimoin DL, Connor JM, Pyeritz RE, Korf BR, editors. *Emery and Rimoin's Principles and Practice of Medical Genetics*, 4th ed. London: Churchill Livingstone. pp299–409.

Wallace DC, Lott MT, Brown MD, Kerstann K. Mitochondria and neuro-ophthalmological diseases. 2001. In: Scriver CR, Beaudet AL, Sly WS, Valle D, editors. *The Metabolic and Molecular Basis of Inherited Disease*, 8th ed. New York: McGraw-Hill. pp2425–2512.

Wallace DC, Lott MT, Procaccio V. 2007. Mitochondrial genes in degenerative diseases, cancer and aging. In: Rimoin DL, Connor JM, Pyeritz RE, Korf BR, editors. *Emery and Rimoin's Principles and Practice of Medical Genetics*, 5th ed. Philadelphia: Churchill Livingstone Elsevier. pp194–298.

Wallace DC, Ruiz-Pesini E, Mishmar D. mtDNA variation, climatic adaptation, degenerative diseases, and longevity. *Cold Spring Harb Symp Quant Biol.* 2003; 68:479–486.

Wallace DC, Singh G, Lott MT, et al.. Mitochondrial DNA mutation associated with Leber's hereditary optic neuropathy. *Science.* 1988a; 242: 1427–1430.

Wallace DC, Zheng X, Lott MT, et al. Familial mitochondrial encephalomyopathy (MERRF): Genetic, pathophysiological and biochemical characterization of a mitochondrial DNA disease. *Cell*. 1988b; 55:601–610.

Wittig I, Braun HP, Schägger H. Blue native PAGE. *Nat Protoc*. 2006; 1(1): 418-428.

Wong LJ, Naviaux RK, Brunetti-Pierri N, et al. Molecular and clinical genetics of mitochondrial diseases due to POLG mutations. *Hum Mutat*. 2008; 29: E150–E172.

Wu CW, Yin PH, Hung WY. Mitochondrial DNA mutations and mitochondrial DNA depletion in gastric cancer. *Genes Chromosom Cancer*. 2005; 44: 19–28.

Yadava N, Houchens T, Potluri P, Scheffler IE. Development and characterization of a conditional mitochondrial complex I assembly system. *J Biol Chem*. 2004; 279: 12406–12413.

Yadava N, Potluri P, Smith EN, Bisevac A, Scheffler IE. Species-specific and mutant MWFE proteins. Their effect on the assembly of a functional mammalian mitochondrial complex I. *J Biol Chem*. 2002; 277: 21221–21230.

Yan H, Parsons DW, Jin G, et al. IDH1 and IDH2 mutations in gliomas. *N Engl J Med*. 2009; 360:765-773.

Yin PH, Lee HC, Chau GY. Alteration of the copy number and deletion of mitochondrial DNA in human hepatocellular carcinoma. *Br J Cancer*. 2004; 90: 2390–2396.

Yu CA, Xia D, Kim H, et al. Structural basis of functions of the mitochondrial cytochrome bc₁ complex. *Biochim Biophys Acta*. 1998 Jun 10;1365(1-2):151-8.

Zeviani M, Antozzi C. Mitochondrial disorders. *Mol Hum Repr*. 1997; 3:133-148.

Zeviani M, Spinazzola A, Carelli V. Nuclear genes in mitochondrial disorders. *Curr Opin Genet Dev*. 2003; 13:1-9.

Zimmermann FA, Mayr JA, Neureiter D, et al. Lack of complex I is associated with oncocytic thyroid tumours. *Br J Cancer* 2009;100:1434 – 7.

Zhu Z, Yao J, Johns T, Fu K, et al. SURF1, encoding a factor involved in the biogenesis of cytochrome c oxidase, is mutated in Leigh syndrome. *Nat Genet.* 1998 ; 20:337–343.

Zuchner S, Mersiyanova IV, Muglia M, et al. Mutations in the mitochondrial GTPase mitofusin 2 cause Charcot-Marie-Tooth neuropathy type 2A. *Nat Genet.* 2004; 36:449–451.

Acknowledgements

This work has been supported by AIRC, *Associazione Italiana Ricerca contro il Cancro*.

Thanks to

Prof. Michela Rugolo, Dipartimento di Biologia Evoluzionistica Sperimentale, Università di Bologna, Italia.

Dr. Anna Maria Porcelli, Dr. Luisa Iommarini, Dr. Maria Antonietta Calvaruso, Dr. Anna Maria Ghelli, Dipartimento di Biologia Evoluzionistica Sperimentale, Università di Bologna.

Dr. Giuseppe Gasparre and Dr. Ivana Kurelac, Dipartimento di Scienze Ginecologiche, Ostetriche e Pediatriche, Genetica Medica, Sant'Orsola-Malpighi, Bologna.

Dr. Claudio Ceccarelli, Unità operativa di Anatomia e Istologia Patologica; Sant'Orsola-Malpighi, Bologna.

Prof. Pier Luigi Lollini, Dipartimento di Ematologia e Scienze Oncologiche, Università di Bologna.

Prof. Christine Betts, Dipartimento di Patologia Sperimentale, Università di Bologna.

Un grazie informale ma sentito a tutto voi che mi sostenete giorno per giorno e con una pazienza infinita: mamma e papà, Mimmo e la sua famiglia, Gaetano e Mattia, Luisa, Claudia, Tania, Martina, Connie ed Annamaria. Mi scuso se qualcuno al momento può essermi sfuggito! Grazie a tutti voi di esserci!

